

CHALMERS



Conduction Band Mediated Charge Transfer for Highly Reduced, Catalytically Active State: A Comparison Between Thin Films and Colloidal Solutions.

Joachim Hedberg

Department of Chemical and Biological Engineering

Division of Physical Chemistry

CHALMERS UNIVERSITY OF TECHNOLOGY

Göteborg, Sweden, 2011

THESIS FOR THE DEGREE OF MASTER OF SCIENCE

Conduction Band Mediated Charge Transfer for Highly
Reduced, Catalytically Active State: A Comparison Between
Thin Films and Colloidal Solutions.

JOACHIM HEDBERG



CHALMERS

Department of Chemical and Biological Engineering

CHALMERS UNIVERSITY OF TECHNOLOGY

Göteborg, Sweden 2011

Conduction Band Mediated Charge Transfer for Highly Reduced, Catalytically Active State:
A Comparison Between Thin Films and Colloidal Solutions.
Joachim Hedberg

© Joachim Hedberg, 2011

Department of Chemical and Biological Engineering
Chalmers University of Technology
SE-412 96 Göteborg
Sweden

Telephone +46(0)31-772 1000

Department of Chemical and Biological Engineering

Göteborg, Sweden 2011

Conduction Band Mediated Charge Transfer for Highly Reduced, Catalytically Active State: A Comparison Between Thin Films and Colloidal Solutions.

JOACHIM HEDBERG

Department of Chemical and Biological Engineering
CHALMERS UNIVERSITY OF TECHNOLOGY

Abstract

In catalysis it is common to use expensive and scarce metals, such as Pt, Ir and Ru, or demand of high energy input, e.g. electroreduction. This work focuses on the possibility of visible light induced catalysis by generation of highly reduced, catalytically active states in a metal porphyrin through conduction band mediation, where the metal is iron or cobalt. To achieve a highly reduced state with visible light one can use a system including a sensitizer, a semiconductor and a catalyst. The sensitizer is used to absorb visible light and inject electrons into the semiconductor, which becomes conducting and mediates electron transfer to the catalyst. The catalyst can be further reduced if the reduction potential of the catalyst and band gap energy of the semiconductor overlaps. When the catalyst is reduced several steps, a multiple electron transfer (MET) catalysis could reduce reactants with a large negative electrochemical potential due to the lowered potential by the use of multiple electrons. This thesis has studied the effect of illumination upon porphyrins anchored to thin films and colloidal particles of TiO₂; and it has been shown that the conduction band mediated charge transfer can occur in thin films of nanocrystalline TiO₂ when iron- or cobalt protoporphyrine IX (PPIX) is bound to the surface. The same effect seem to be absent in nanoparticulate TiO₂. The illumination with UV-light generated a build-up of conduction band electrons which reduced Fe(III) via Fe(II) to Fe(I). The reduction process was monitored and found to be highly regenerative after ended illumination, indicating nearly reversible redox processes. Conduction band electrons were found to be stable when reduction from M(II)PPIX to M(I)PPIX did not occur.

Keywords: conduction band mediation, multiple electron transfer, porphyrin, TiO₂, colloidal solution, thin film.

Abbreviation list / Dictionary

FePPIX	Also known as Hemin (see below)
Hemin	Iron protoporphyrin IX chloride
CoPPIX	Cobalt protoporphyrin IX chloride
MPPIX	Metal protoporphyrin IX chloride (referring to FePPIX or CoPPIX)
TBAPF ₆	Tetrabutylammonium hexafluorophosphate
DMSO	Dimethyl sulfoxide
MET	Multiple electron transfer
FT-IR	Fourier transform infrared (spectroscopy)
VB	Valance band
CB	Conduction band
BG	Band gap
VR	Vibrational relaxation
IC	Internal conversion
ISC	Intersystem crossing

Table of Contents

1. Introduction.....	3
1.1. Background.....	3
1.2. Purpose	6
1.3. Scope of project	6
2. Theory and background	7
2.1. Porphyrins	7
2.1.1. Light's interaction with matter.....	8
2.1.2. Binding of porphyrins to TiO ₂ by carboxylic groups	8
2.2. Semiconductors and conduction band mediated charge transfer	8
2.3. Scattering by nanoparticles.....	10
2.4. Lasers.....	11
3. Method and materials.....	12
3.1. Chemicals	12
3.2. Equipment	12
3.3. UV-Vis absorbance spectroscopy.....	12
3.3.1. Extinction coefficients measurements.....	12
3.3.2. Transient absorbance spectroscopy.....	13
3.4. FT-IR spectroscopy	14
3.5. Preparation of TiO ₂ thin films.....	15
3.6. Experimental procedure of producing and monitoring MPPIX reduced states.....	15
3.7. Studies of the anchoring of porphyrins to TiO ₂ nanoparticles	15
3.8. Heat and ambient light effect upon porphyrins.....	16
4. Results and discussion.....	17
4.1. Extinction coefficient study of MPPIX in different solvents.....	17
4.2. Porphyrins in neat solutions.....	18
4.3. Porphyrins in colloidal solutions	21
4.4. Porphyrins anchored to TiO ₂ thin films.....	26
4.5. Anchoring of porphyrins to nanoparticular TiO ₂	31
4.6. Nanoparticular TiO ₂ in neat solution.....	32
4.6.1. Illumination of TiO ₂ in neat solvent.....	32
4.6.1. Sedimentation of TiO ₂ in neat methanol	32

5. Discussion.....	33
6. Summary and outlook.....	34
6.1. Summary	34
6.2. Outlook.....	34
7. Acknowledgements.....	35
References.....	36
Appendix – Extinction coefficients.....	37
CoPPIX in DMSO	37
CoPPIX in methanol.....	38
CoPPIX in pyridine	39
FePPIX in pyridine.....	40

1. Introduction

1.1. Background

As the anthropogenic contribution to CO₂ in the atmosphere is climbing, accompanied by deforestation^[1], there is a growing demand for carbon-neutral energy sources as well as means of reducing the emissions of CO₂ to the atmosphere.

Various methods of lowering the levels of CO₂ have been suggested; e.g. trapping in other compounds, storage in gas pockets and electroreduction of CO₂ into other compounds. Trapping requires a lot of liquid/solid material, storage is very energy demanding, as is electroreduction. Because the reduction potential of CO₂ in single electron reactions is fairly high (see reaction 1 Table 1), it's hard to chemically reduce it. The reduction potential is far less in the cases where multiple electrons is involved; see examples in Table 1, reaction 2-7. However, multiple electron transfer (MET) with coupled proton transfer reactions is more complicated than single electron transfer events and thus, the parameters governing MET is of great interest for catalysis.

Table 1: Electrochemical potential of reactions for reducing carbon dioxide^[2].

	Reaction	Potential vs SCE at pH 7
1	$\text{CO}_2 + \text{e}^- \rightarrow \text{CO}_2^{\bullet -}$	-2.14 V
2	$\text{CO}_2 + 2\text{H}^+ + 2\text{e}^- \rightarrow \text{HCO}_2\text{H}$	-0.85 V
3	$\text{CO}_2 + 2\text{H}^+ + 2\text{e}^- \rightarrow \text{CO} + \text{H}_2\text{O}$	-0.77 V
4	$\text{CO}_2 + 4\text{H}^+ + 4\text{e}^- \rightarrow \text{C} + 2\text{H}_2\text{O}$	-0.44 V
5	$\text{CO}_2 + 4\text{H}^+ + 4\text{e}^- \rightarrow \text{HCHO} + \text{H}_2\text{O}$	-0.72 V
6	$\text{CO}_2 + 6\text{H}^+ + 6\text{e}^- \rightarrow \text{CH}_3\text{OH} + \text{H}_2\text{O}$	-0.62 V
7	$\text{CO}_2 + 8\text{H}^+ + 8\text{e}^- \rightarrow \text{CH}_4 + 2\text{H}_2\text{O}$	-0.48 V

If we are able to understand and control efficient visible light induced MET reactions, we could convert CO₂ into other compounds, e.g. methanol or formaldehyde; furthermore, if these reactions could be initiated with visible light, no external input to start the MET catalysis would be needed. The use of visible light is preferred as it constitutes the most energy intense part of the Earth's received radiation at sea level, see Figure 1.

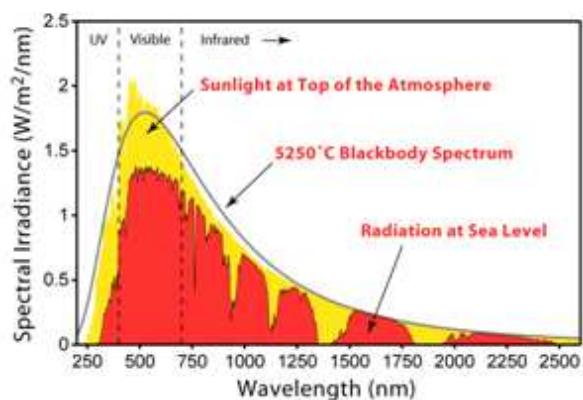


Figure 1, Solar radiation spectrum depicting the energy of incoming light of different wavelengths above the atmosphere (yellow) and at sea level (red); modified picture of American Society for Testing and Materials (ASTM) Terrestrial Reference Spectra.

Visible light catalysis can be carried out by excitation of sensitizer molecules which can inject electrons into a semiconductor, e.g. nanocrystalline TiO_2 (like in dye-sensitized solar cells), followed by conduction band mediated charge transfer from the semiconductor to the catalyst moiety; see Figure 2 for illustration. Visible light can also promote valence band electrons to the conduction band of the semiconductors conduction band if the band gap energy is tuned to correspond to the energy of the light^[3]. Nanoparticulate TiO_2 is a photoconductor, but the wavelength needed corresponds to UV-light which is less intense at sea level. The purpose of sensitizers is to red shift the wavelengths needed to generate conduction band electrons. It's been proven possible to build up a concentration of conduction band electrons in semiconductors^[4], which in turn can be used for producing the highly reduced, catalytically active state of the catalyst via conduction band mediation.

With the correct specificity and availability of protons, the highly reduced catalyst can ideally, through MET, reduce CO_2 into the products in Table 1 (reaction 2-7). Depending on the state of reduction of the catalyst, some reactions are less probable than others; catalysts able to reduce CO_2 is likely to also reduce H^+ to H_2 , which raise a demand of selective catalysis as we do not intend to produce H_2 ^[5]. Even if we can circumvent the generation of H_2 , it is possible that the reduction of e.g. one carbon dioxide into one methane and two water molecules is one of the reaction less likely to occur due to the large number of electrons involved, despite the rather low reduction potential. It has previously been shown that using different metal deposited at the TiO_2 surface may increase yield and selectivity of photocatalytic CO_2 reduction^[6].

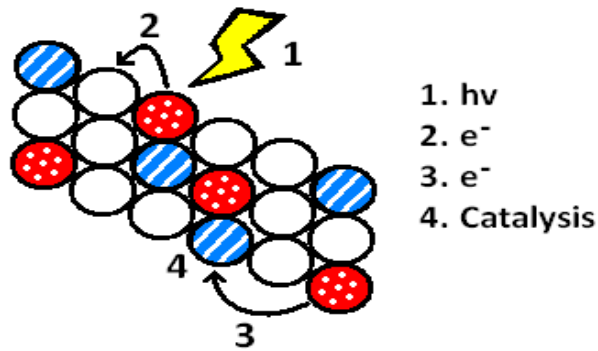


Figure 2, Schematic description of the ideal, light driven conduction band mediated catalysis. (1) Light hits one of the sensitizer molecules (red/dotted) attached to the nanocrystalline TiO_2 , (2) this compound inject an electron into the TiO_2 -array (white). (3) Electrons from the TiO_2 are transferred to the catalyst and reduces it (blue/striped) (4) which perform the catalysis.

It has been shown that the conduction band level, E_{cb} , of nanocrystalline TiO_2 can be tuned relative to the reduction potential of the molecules attached to the surface^[7]. The ground and excited state reduction potentials of an anchored molecule are also, but to lesser extent, affected by electrolytes. Hence, it is possible to tune interfacial energetics, which is needed if we want both injection of electrons into TiO_2 from the sensitizers and the charge transfer from TiO_2 into the catalyst. This demand is raised due to electron injection's need of overlap of the conduction band and the reduced and oxidized form of the anchored molecule^[4].

1.2. Purpose

This project is a small part of a long-term research plan aimed to;

- Establish understanding and subsequent control of the factors governing conduction band mediated charge transfer processes.
- Testing and modifying catalyst and its environment in combination with the anchored sensitizer to optimize the conditions for MET.
- Apply this knowledge in the design of molecular-materials assemblies capable of performing visible light-induced MET photo catalysis.

The main purpose of this master thesis project deal with the first of the goals stated above, and is focused on understanding and optimizing the conduction band mediated generation of catalytically active states of iron and cobalt porphyrin anchored to thin films and colloidal particles of nanocrystalline TiO₂, and especially to investigate whether thin films or colloidal solutions is the better alternative.

1.3. Scope of project

This project has investigated the influence of different conditions on the photoinduced generation of highly reduced states of iron and cobalt protoporphyrin IX. Those porphyrins possesses several desirable properties as model molecules for deeper understanding of conduction band mediated processes; e.g. photostability, resistance against heat decomposition, stability in solution^[8] and high extinction coefficients with large difference between redox states^[9]. The investigated conditions are:

- Solvents
 - DMSO
 - Water
 - Methanol
 - Ethanol
 - Pyridine
- Additives
 - Lithium perchlorate
 - Tetrabutylammonium hexafluorophosphate
- Semiconductor arrangement
 - Neat solution for reference
 - Colloidal solution
 - Thin film
- Illumination parameters
 - Time
 - Continuous/pulses
 - Wavelength

2. Theory and background

2.1. Porphyrins

Porphyrins are versatile molecules, crucial for life as we know it; they are in the centre of the photosynthesis, as chlorophyll, and in our oxygen transporting protein hemoglobin, as heme, which also is known as iron protoporphyrin IX (FePPIX)^[10]. The least denominator of all porphyrins is the four pyrrol units connected to one another at each side of the nitrogen, resulting in a macro cycle with 20 carbon units in the other ring, see Figure 3. The highly aromatic structure usually has a central metal atom, in this thesis it constitutes of cobalt and iron; porphyrins lacking this central metal atom are known as free-base porphyrins.



Figure 3, An illustration of Metal Protoporphyrin IX; M is, in this thesis, either Fe or Co.

A metal porphyrin can usually coordinate one or two ligands axially which can greatly affect the perceived color of the molecule; for instance, oxygenated FePPIX is bright red while deoxygenated FePPIX in DMSO is dark green. The color shift induced by changing ligand is due to the metal to ligand charge transfer (MLCT) energy, which is in the same range as the energy of visible light. This shift is also very pronounced in an absorption spectrum, where the dominant peak (Soret band) usually experience a red or blue shift upon solvent change^[11].

The Soret band of porphyrins is situated around 400 nm and is far stronger than the Q-band, which usually constitutes of a broad band with two small peaks in the 500-600 nm range, see Figure 4. When the porphyrin is reduced from e.g. 3+ to 2+ the spectra also shifts as the energy levels of the molecule changes^[8].

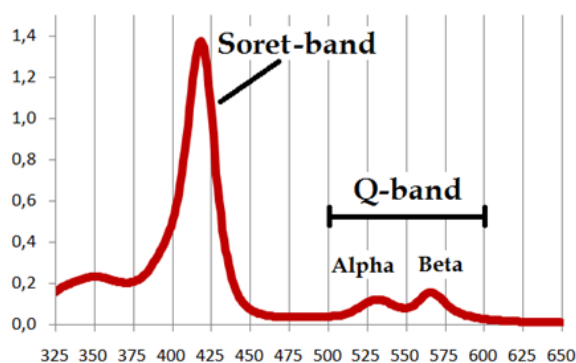


Figure 4, Illustration of a typical porphyrin spectrum with the Soret band and Q-band (with the smaller peaks called Alpha and Beta).

2.1.1. Light's interaction with matter

When light interact with matter, several possible pathways of de-excitation are possible, this is usually depicted in a Jablonski diagram, see Figure 5. Absorbance (A), fluorescence (F) and phosphorescence (P) are the radiative pathways while the vibrational relaxation (VR), internal conversion (IC) and inter system crossing (ISC), are non-radiative.

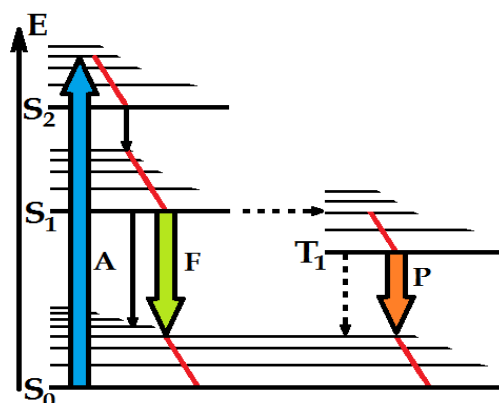


Figure 5, Jablonski diagram; blue arrow labeled A represent absorption from the ground state (S_0) to an excited state (S_1 , S_2 etc), red lines corresponds to vibrational relaxation (VR) to the electronically excited state, black arrows internal conversion (IC), black dashed arrows inter system crossing (ISC), F represent fluorescence and P phosphorescence.

When a molecule have an overlap between its energy levels and the wavelength of light, absorption is possible; if the energy is high enough an electronic excitation puts the molecule at S_1 , S_2 or a higher electronic state. The molecule goes through a rapid vibrational relaxation possibly followed by internal conversion, fluorescence from the S_2 or higher states is rarely seen (and is therefore not depicted in Figure 5).

2.1.2. Binding of porphyrins to TiO_2 by carboxylic groups

The binding character of MPPIX to TiO_2 is widely discussed in the scientific community, however, consensus states that the carboxylic groups of MPPIX attaches to the TiO_2 ^[12], such that a change should affect the carboxylic groups IR-signal. The anchoring of MPPIX can therefore, in principle, be monitored by IR-spectroscopy, examining the acid spectral regions.

FT-IR spectroscopy is, in theory, ideal for monitoring those kind of changes, however, there are problems with the method when applied to very low concentrations in solution; and the solubilized particles and complexes is what is interesting for the purpose of this thesis.

2.2. Semiconductors and conduction band mediated charge transfer

A semiconductor is a material that has, in its ground state, a filled valance band (VB) and an empty conduction band (CB). Based on those properties it's an insulator, but it can however become conductive if electrons from the valance band are promoted to the conduction band. This can be done with e.g. heat and this is the reason why semiconductors become more conductive with temperature, while metals display an inverse relationship between temperature and conductivity. Semiconductors can also become conductive when illuminated,

a phenomenon called photoconductivity. If the energy of the light corresponds to the band gap energy, electrons can be promoted to the conduction band^[3], see Figure 6.

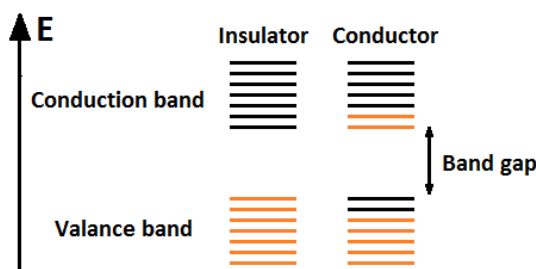


Figure 6, Energy levels of a semiconductor. To the left, the ground state of the material (insulating). To the right, electrons promoted to the conduction band (conducting).

In this thesis TiO₂ is used, more specifically anatase nanoparticles, either in colloidal solutions or as TiO₂ past for film making. When crystal structures are on the macroscopic scale, the number of allowed energy levels in the material is huge, basically infinite; however, as the crystals become smaller the atomic properties become more pronounced. This means the particle size affects the band gap energy, were a decrease in size results in a larger band gap. A macro-sized crystal has far more allowed energy states, with a lot of equally leveled energy bands (degeneracy), which results in continuous bands (both VB and CB); the particles band energies are more discrete in nature (and therefore also known as quantum dots)^[3], see Figure 7.

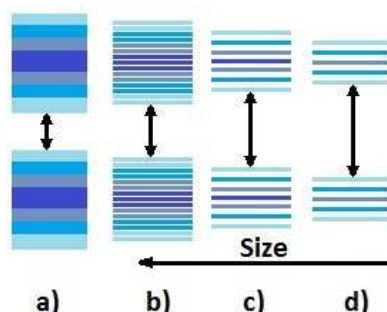


Figure 7, Energy bands for continuous material (a) and nanoparticles with decreasing size ($b > c > d$) with band gap energy in order $a < b < c < d$. For the energy levels, dark color corresponds to high degeneracy while pale color indicates few allowed energy levels.

As the electron population of the conduction band increases, they become visible in absorbance spectroscopy; in TiO₂, conduction band electrons, so called “hot electrons”, have a broad absorption from ~500 to over 1100 nm^[5b, 13]. When the band energy of this state overlap with the reduction potential of an anchored molecule, it’s possible that an electron transfer to that species occurs^[4]; actually overlap of energy levels is *crucial* for the electron transfer to take place^[4]. That means one either needs to find a perfect match of anchored molecule and semiconductor or try to manipulate the conduction band of the latter. It is clear that the conduction band can be tuned slightly by altering particle size, further fine tuning by addition of electrolytes has also been proven possible^[14].

The largest effect is acquired when small cations, so-called potential determining ions e.g. H^+ , Li^+ and Mg^{2+} , is added; which results in a substantial decrease of the conduction band level, resulting in higher rate of sensitizer injection to the TiO_2 ^[4, 7, 14]. However, this can cause less overlap with the redox potential of the catalyst, which is necessary for effective conduction band mediation. Those small cations has also been proven to improve Fe(0)Porphyrin's lifetime and catalytic efficiency^[15].

The use of $TBAPF_6$ is motivated as supporting electrolyte, in addition to tuning the CB, inert in the system^[14].

2.3. Scattering by nanoparticles

Colloidal solutions give rise to lower transmittance due to scattering, resulting in a lower registration of light intensity and hence a higher absorbance. According to Rayleigh scattering theory the scattering is proportional to $(1/\lambda^4)$, an illustration of this can be seen in Figure 8. Rayleigh scattering is a reasonably accurate estimation of the scattering as long as the particle size is less than one tenth of the wavelength; in this project, particles of 25 nm in diameter was used for colloidal particles and 15-20 nm for thin films.

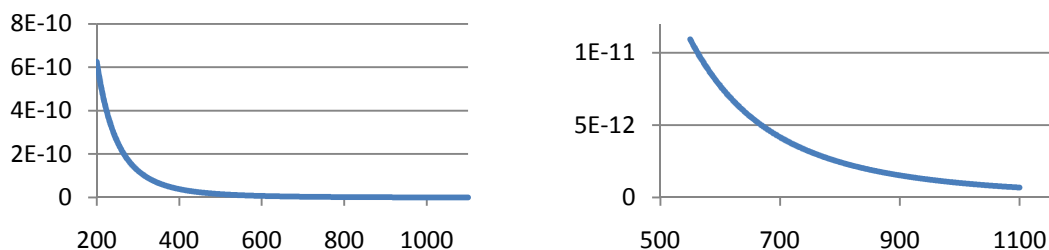


Figure 8, Plot of $(1/\lambda)^4$ versus λ (nm), depicting the relative scattering power between different wavelength. To the left is represented the whole region of interest of this project and to the right the region 550-1000 are enlarged.

Any aggregation of nanoparticles would show a decrease in scattering over the whole range of the spectra, as the number of particles decreases. However, the lower wavelengths are submitted to, at first, a greater decrease in absorbance as the size of the aggregates surpass one tenth of the wavelength; if the aggregation continues, the longer wavelengths will be affected to the same extent.

The Rayleigh scattering model poorly describes the scattering by larger particles, which is better explained by the Mie scattering model. Mie scattering is less wavelength dependent and more dependent on incident light angle which gives rise to a less affected spectrum as the largest part of the scattered light is directed in the lights path; the larger the particles, the greater the scattering in forward direction.

2.4. Lasers

Lasers are used to get an intense, monochromatic and coherent beam of light with small divergence. This is done by pumping an active medium (AM), e.g. a Nd:YAG; pumping is the process of excitation of the medium molecules to a higher state either directly or by another excited state, i.e. an n-level laser, where n could be e.g. 3 or 4. The excitation method is executed either by a high voltage system or by photo excitation; this is done to achieve what is called population inversion (PI). PI occurs when an excited state is more populated than the ground state; this leads to the possibility of light amplification by the stimulated emission of radiation, or LASER. One excited molecule emits radiation of a specific wavelength as it falls back into the ground state; this radiation induced a stimulated emission from another molecule resulting in 2 photons and so on^[16].

The chain reaction achieved is directed between two mirrors (M_1 and M_2) with a distance (d) equals an integer number times the half wavelength of the emission (to keep the radiation in phase)^[16]; see Figure 9 for illustration of setup.

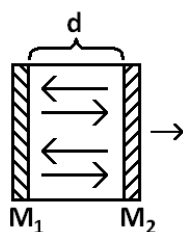


Figure 9, Simple illustrative laser setup.

Mirror 1 and 2 are constructed of very highly reflective mirrors, but M_2 is constructed to allow a small amount of the radiation to leak out to be used in some application.

To get a higher power laser output one can charge up the laser compartment, by a method called Q-switching, during a shorter time and then release the energy to gain high energy short pulses instead of a continuous light beam. The use of laser pulses is a very useful tool when studying fast kinetics and is used to study processes down to the femtosecond time scale.

3. Method and materials

3.1. Chemicals

The chemicals used during the project are listed below:

- Metal protoporphyrin IX complexes (MPPIX)
 - Iron protoporphyrin IX complex (FePPiX) [$\geq 98\%$ (HPLC), Sigma]
 - Cobalt protoporphyrin IX complex (CoPPiX) [Aldrich #C1900]
- Titanium dioxide (anatase) paste, for thin film making [15-20 nm particle diameter, ~11wt%, Ti-nanoxid T20, Solaronix]
- Titanium dioxide (anatase) particles [< 25 nm particle diameter, 99.7%, Aldrich]
- Lithium perchlorate (LiClO_4) [$\geq 99.0\%$, Fluka]
- Tetrabutylammonium hexafluorophosphate (TBAPF_6) [98%, Aldrich]
- Dimethyl sulfoxide (DMSO) [$\geq 99.9\%$, Sigma-Aldrich]
- Methanol [$\geq 99\%$, Sigma-Aldrich]
- Ethanol [96%, Etax, Solveco AB]
- Pyridine ($\text{C}_5\text{H}_5\text{N}$) [$\geq 99.5\%$, Riedel-de Haën]

Solvents, nanoparticulate TiO_2 and salts were used as received.

3.2. Equipment

The equipment used during the project are listed below:

- 2 different Varian Cary 50 Bio UV-Visible Spectrophotometer
- 2 different Xe-lamps (one using filters, one using a monochromator)
- Spex 1681 0.22 m Spectrometre (monochromator)
- Continuum Surelite (laser)
- Surelite SSP (beam splitting unit)

3.3. UV-Vis absorbance spectroscopy

UV-Vis spectroscopy is used to determine the absorption of the samples at different wavelengths. The absorbance, A , of the sample is a factor of the extinction coefficient at the specific wavelength, ϵ_λ , the concentration of the species in the sample, c , and the path length of the light, b . Absorbance is a measure of the light that does not pass through the sample and corresponds to the base ten logarithm of incident light, I_0 , divided by light registered by the detector, I . This is known as Lambert-Beers law which is written as:

$$A = \log_{10} \frac{I_0}{I} = \epsilon_\lambda cb$$

3.3.1. Extinction coefficients measurements

The extinction coefficients of different substances can be determined by establishing the relation between absorbance and concentration. Linear regression on the chosen wavelength will give a slope of the graph that correspond to the extinction coefficient of the molecule at that wavelength, see Figure 10.

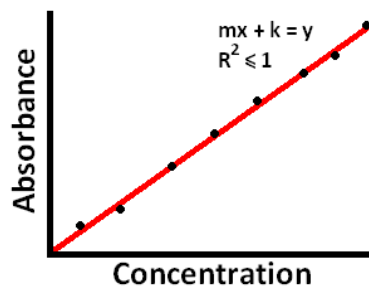


Figure 10, Example of titration experiment for determination of extinction coefficient. m equals the extinction coefficient, ideally k should equal zero while R^2 equals one.

3.3.2. Transient absorbance spectroscopy

Transient absorption spectroscopy is a method of quantifying photoinduced changes by illuminating a sample with a pump light or laser and continually measuring the resulting absorbance; changes to the sample registered are a function of time and incident light. The illumination pathway is perpendicular to the probe beam to avoid light from the probe light in the detector; see Figure 11. Transient absorption is normally used for monitoring excited state reaction of the fs-ms time-scale, but in this project, even longer-lived transient species are examined.

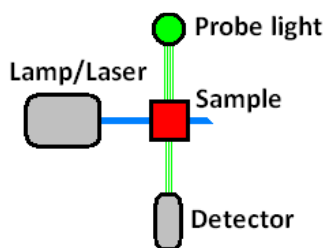


Figure 11, An example of transient absorption spectroscopy experimental setup.

The absorption of the initial sample is measured and used as a baseline for the light induced state's absorption spectrum, effectively measuring the difference in absorption (Δ Abs) as a function of time, pump light intensity and excitation wavelength; Figure 12 gives an example of a principal spectra.

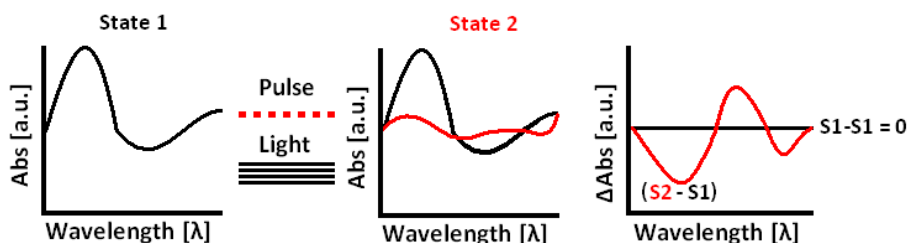


Figure 12, Example of transient absorption spectra. From the left; an initial sample (State 1), not illuminated, is recorded for comparison. A pump light or laser pulses is directed through the sample and the illuminated sample is recorded (State 2); the result is a difference spectra depicting the change in absorption as a function of illumination time/pulse count.

The subtraction of the initial spectra from the resulting state gives a difference spectra where the changes are easier to follow. When two or more measurements coincide at some wavelength, that wavelength constitutes an isosbestic point; which arise from the fact that the extinction coefficients of state 1 and 2 are equal. In Figure 12 the isosbestic points are positioned where the red line crosses the black; which can be seen in both the middle and rightmost picture. Those points can be used to calculate the total concentration of a sample when the ratio of state 1 and 2 is unknown; if the isosbestic points are not maintained it is due to destruction of the molecule or the generation of further states.

3.4. FT-IR spectroscopy

Fourier transform infra red spectroscopy (FT-IR) gives information about the vibrational energy of the molecules in a sample, i.e. absorbance in the infrared region. By a complex array of mirrors and lenses one receives a result as an interferogram; which, by applying a Fourier transform (FT), is converted into a spectrum with absorbance versus wavelength^[17], see Figure 13.

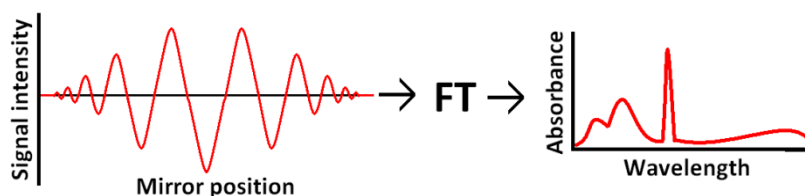


Figure 13, Illustration of FT-IR raw data to spectrum procedure.

Changes involving groups with strong absorbance in the IR-region, e.g. carboxylic groups, can easily be seen in an FT-IR experiment. If the carboxylic group binds to another species the vibration energy would change and intensity in the carboxylic range would decrease proportional to the ratio of bound functional groups.

In this project the complexes studied have two carbon chains with carboxylic groups and FT-IR can be used to monitor if none, one or both groups bind to the TiO_2 (assuming same number of bonds for all complexes); or more correctly, the average number of bonds per porphyrin.

FT-IR measurements are nevertheless not unproblematic; solvents can have strong absorbance in the same region as they often contain groups with similar IR-absorption (e.g. $-\text{OH}$, $\text{S}=\text{O}$). Furthermore, the concentration of the molecule to be examined might not be soluble to the extent were it becomes detectable, which is troubling as oversaturated or non soluble amount might distort the results. If the vapor pressure of the solvent is moderate, it is possible to evaporate it to get a less drenched signal from the studied molecule; however, again, this might greatly distort the results.

3.5. Preparation of TiO₂ thin films

The TiO₂ thin films were prepared by lining up glass slides, taped together with Scotch tape, addition of a small amount of TiO₂ paste at one end and pressed out with a glass rod (“doctor-blading”), see Figure 14. This produced smooth, thin films with a thickness equal to that of tape used. The TiO₂ were allowed to dry for 30 min before they were heated to 400°C for 30 min; this was to allow the TiO₂ to attach better to the surface of the glass slides and to evaporate solvent.

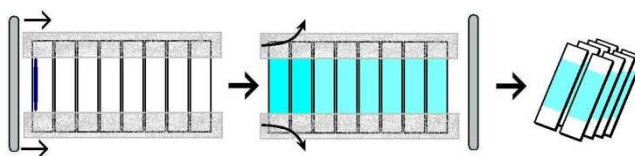


Figure 14, Simple illustration of the doctor-blading procedure; blue represents the TiO₂ solution.

To dye the films, they were immersed in MPPIX solution, either for a certain time or to a specific absorption; they were subsequently rinsed with the same solvent to remove excess, unbound porphyrins and then placed in cuvettes filled with solvent and electrolyte if applicable.

As films were, to some degree, inhomogeneous with respect to thickness and anchored porphyrins, they needed to be stationary during measurements to obtain quantitative results.

3.6. Experimental procedure of producing and monitoring MPPIX reduced states

Light induced changes to MPPIX in solution, anchored to colloidal particles and to TiO₂ thin films were monitored with transient absorbance spectroscopy; thin film and colloidal particles were also measured without porphyrins as reference.

Four different illumination sources were used; a Nd-YAG laser for pulsed illumination experiments, a high intensity Xe-lamp in combination with filters for broad illumination, a Xe-lamp with a monochromator for single wavelength illumination and a fluorescent tube for ambient light stability tests.

The porphyrin samples were illuminated with different setups and measured over time to evaluate the kinetics of the light induced changes.

3.7. Studies of the anchoring of porphyrins to TiO₂ nanoparticles

The anchoring of porphyrins to TiO₂ was examined in two different manners:

- FT-IR – Proof of anchoring of MPPIX to TiO₂ by carboxylic groups.
- Transient absorption spectroscopy - Monitoring changes in the absorbance over time when TiO₂ is introduced into a system containing MPPIX.

Neat solvent, MPPIX in solvent and MPPIX anchored to TiO₂ particles were examined with FT-IR, as well as samples containing MPPIX and TiO₂ anchored MPPIX in ethanol where the solvent

was evaporated. Due to reasons explained in the theory section concerning FT-IR; no good measurement of MPPIX in its environment was obtained, probably due to the low concentration of porphyrin in the samples.

Ocular examination of the thin films also makes it easy to say there were in fact anchored porphyrins to the TiO₂.

Further examination was performed to see how the sedimentation affected the solution. It was carried out by monitoring of sedimentation and aggregation effect upon the absorbance when colloidal solution was stored and its ability to recover to the initial state; i.e. rigorously shaking/mixing sample to see if the process is reversible.

3.8. Heat and ambient light effect upon porphyrins

The protoporphyrin's resilience towards ambient environments was examined with absorbance spectroscopy, the different experiments was carried out as follows:

- Ambient environment – Sample were put in ambient light and temperature over time and measured with absorbance spectroscopy.
- Simultaneous temperature and light experiment – Sample put under table lamp with and without ice bath and monitored with absorbance spectroscopy.

4. Results and discussion

4.1. Extinction coefficient study of MPPIX in different solvents

Aliquots of FePPIX and CoPPIX in different solvents were performed to receive data on the extinction coefficients; CoPPIX in methanol was performed as a titration experiment. The three graphs below depicts FePPIX in DMSO, illustrating the principal approach of extinction coefficient determination, see Figure 15. The remaining graphs are viewable in Appendix. The R^2 values are rounded up to 1 by the program after four consecutive decimals of nines.

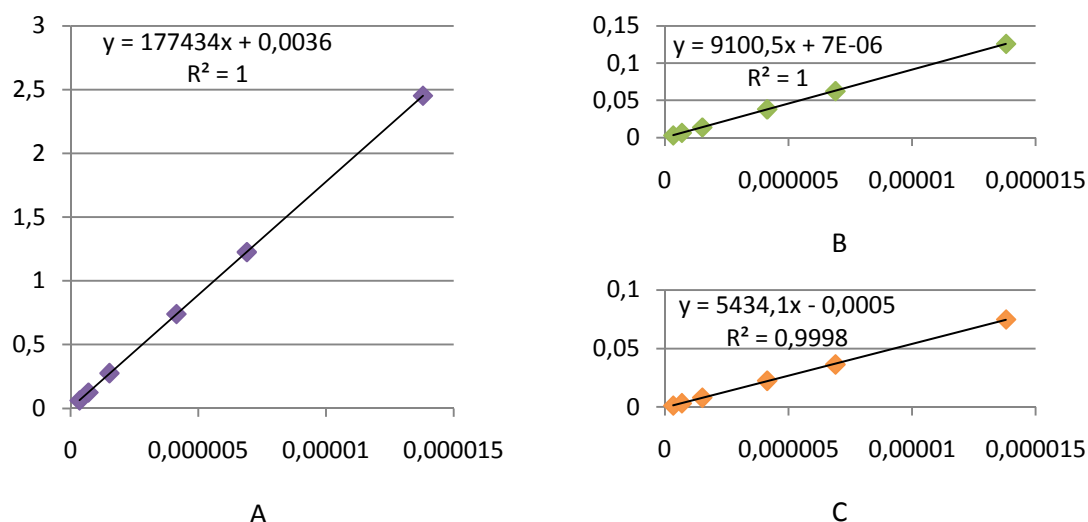


Figure 15, Linear regression of absorbance versus concentration (mol/dm^3) for FePPIX in DMSO for different wavelengths; A: Soret band (404 nm) B: Alpha band (501 nm) C: Beta band (625 nm).

The extinction coefficients of the porphyrins in different solvents are presented below in Table 2 (FePPIX) and Table 3 (CoPPIX):

Table 2: Extinction coefficients of FePPIX in different solvents, maximum of peak in brackets.

Solvent	$\epsilon_{\text{Soret}} (\times 10^3 \text{M}^{-1})$	$\epsilon_{\text{Alpha}} (\times 10^3 \text{M}^{-1})$	$\epsilon_{\text{Beta}} (\times 10^3 \text{M}^{-1})$	$\epsilon_{\text{Shoulder}} (\times 10^3 \text{M}^{-1})$
DMSO	177 [404 nm]	9.10 [501 nm]	5.43 [625 nm]	-
Pyridine*	306 [427 nm]	27.3 [536 nm]	26.7 [570 nm]	55.3 [259 nm]

* Pyridine samples were measured a week after mixing to achieve total solubilization; pyridine sample porphyrin seems to, a large extent, have undergone a reduction to +2.

Table 3: Extinction coefficients of CoPPIX in different solvents, maximum of peak in brackets.

Solvent	$\epsilon_{\text{Soret}} (\times 10^3 \text{M}^{-1})$	$\epsilon_{\text{Alpha}} (\times 10^3 \text{M}^{-1})$	$\epsilon_{\text{Beta}} (\times 10^3 \text{M}^{-1})$	$\epsilon_{\text{Shoulder}} (\times 10^3 \text{M}^{-1})$
DMSO	303 [424 nm]	32.9 [535 nm]	36.6 [569 nm]	64.1 [356 nm]
MeOH	93.3 [418 nm]	8.23 [531 nm]	10.6 [565 nm]	15.8 [351 nm]
Pyridine*	116 [427 nm]	10.2 [537 nm]	9.90 [571 nm]	20.3 [259 nm]

* Pyridine samples were measured a week after mixing.

Extinction coefficients in literature have been hard to find for CoPPIX while FePPIX is studied to a greater extent. Literature values of FePPIX can be seen in Table 4^[9]. A comparison between

literature values to the experimental data hints that a mixture of redox states was present in pyridine; both the wavelength position of the Soret band and the extinction coefficient match $(\text{Py})_2\text{Fe(II)PPIX}$ better than $(\text{Py})_2\text{Fe(III)PPIX}^{[9]}$, assuming similar extinction coefficients in solution and bound to nanoparticulate TiO_2 ^[18].

Table 4: Literature values for extinction coefficients of $\text{FePPIX}^{[9]}$, maximum of peak in brackets. *S* stands for solvent.

$[(\text{S})_2\text{Fe(III)PPIX}]^+$			
Solvent	$\epsilon_{\text{Soret}} (\times 10^3 \text{M}^{-1})$	$\epsilon_{\text{Alpha}} (\times 10^3 \text{M}^{-1})$	$\epsilon_{\text{Beta}} (\times 10^3 \text{M}^{-1})$
DMSO	[424 nm]	[498 nm]	[624 nm]
DMSO/ TiO_2	140 [394 nm]	[535-660 nm broad abs]	
MeOH/ TiO_2	145 [395 nm]	[480 nm]	[600 nm]
Pyridine/ TiO_2	142 [396 nm]	[535-660 nm broad abs]	
$(\text{S})_2\text{Fe(II)PPIX}$			
Solvent	$\epsilon_{\text{Soret}} (\times 10^3 \text{M}^{-1})$	$\epsilon_{\text{Alpha}} (\times 10^3 \text{M}^{-1})$	$\epsilon_{\text{Beta}} (\times 10^3 \text{M}^{-1})$
DMSO	[424 nm]	[525 nm]	[557 nm]
DMSO/ TiO_2	316 [423nm]	[528 nm]	[556 nm]
MeOH/ TiO_2	156 [416 nm]	[495-625 nm broad abs]	
Pyridine/ TiO_2	330 [419 nm]	[526 nm]	[557 nm]

When the spectra are normalized they should, and did, interlace perfectly. However, in the UV-region, where the porphyrins are less absorbing, there are deviations; the same pattern is present in both FePPIX and CoPPIX samples in DMSO, methanol and ethanol, but not in pyridine. This could indicate that axial coordination to the oxygen in the solvent is responsible for this behavior; although, this does not affect our wavelengths of interest and does not distort the main results.

4.2. Porphyrins in neat solutions

Addition of porphyrins to neat solvent was performed with water, DMSO, methanol and pyridine. The experiments using water as solvent were of little use since the solubility of MPPIX in water is very low; even excessive adding and mixing showed only barely detectable traces of porphyrins on the spectrophotometer.

When FePPIX and CoPPIX were illuminated in neat solvent, the amount of reduced FePPIX was lesser than the amount of reduced CoPPIX ; in both cases the amount of reduced porphyrin was small and the rate of reduction slow. CoPPIX was also observed to be more photostable than FePPIX (see Figure 16, Figure 18 and Figure 19), and the overall trend implies that CoPPIX is considerably more viable for photoreduction in non-colloidal solvents, see Figure 16 for comparison in methanol; similar results are retrieved with DMSO as solvent. It has previously been shown that FePPIX in DMSO is photolabile^[19] and that the photodecomposition rate might be speeded up by higher concentration of the porphyrin^[20].

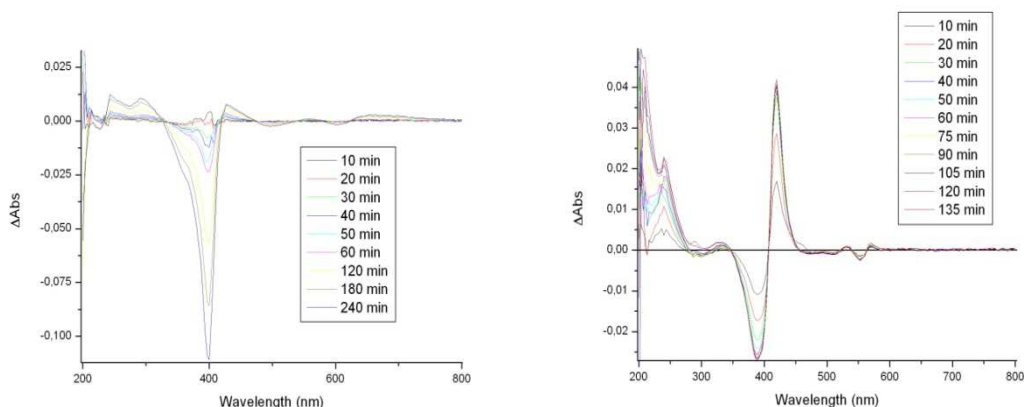


Figure 16, Differential spectra of illuminated of FePPIX (left, max abs 1.25) and CoPPIX (right, max abs 0.55); monochromatic 295 nm light used first 60 min, the wavelength was then lowered to 275 nm.

Furthermore, the rate of solubilization, at least in methanol, DMSO and water, are several orders of magnitude higher for CoPPIX than FePPIX. While CoPPIX dissolves readily, and can be measured accurately almost instantly after mixing, FePPIX can take up to 24 hours before it is completely solubilized, see Figure 17.

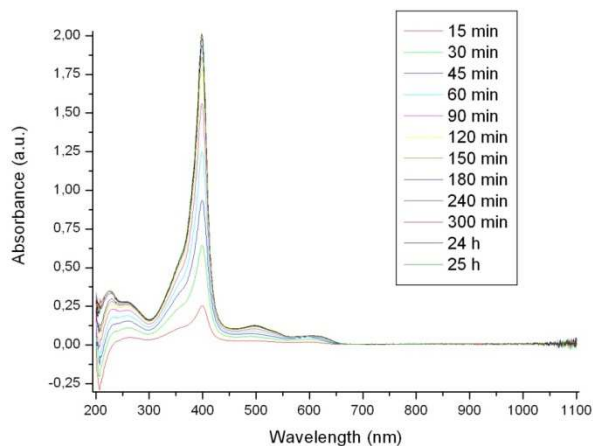


Figure 17, Solubilization curve of FePPIX added to methanol purged with N_2 .

When light induced reduction of FePPIX in methanol and DMSO was performed, with monochromatic light from a Xe-lamp, some red shift of the Soret band was observed, indicating reduction; there was also observed destruction of the porphyrins. The timescale in the initial experiments were different than those performed later on (i.e. colloidal solution and film experiments), which means more information can be obtained.

The CoPPIX samples got reduced from Co(III) to Co(II) in all of the solvents, except in water, where illumination was not performed due to the poor solubility; the means of illumination were a Nd:YAG pulsed laser (355 nm) and monochromatic light from Xe-lamp.

Experiments also indicate that CoPPIX is more photostable than FePPIX under warm illumination ($\sim 45^\circ$), see Figure 19, and suffered about a third less destruction. Under cooled illumination the stability of the porphyrins was fairly similar, see Figure 18.

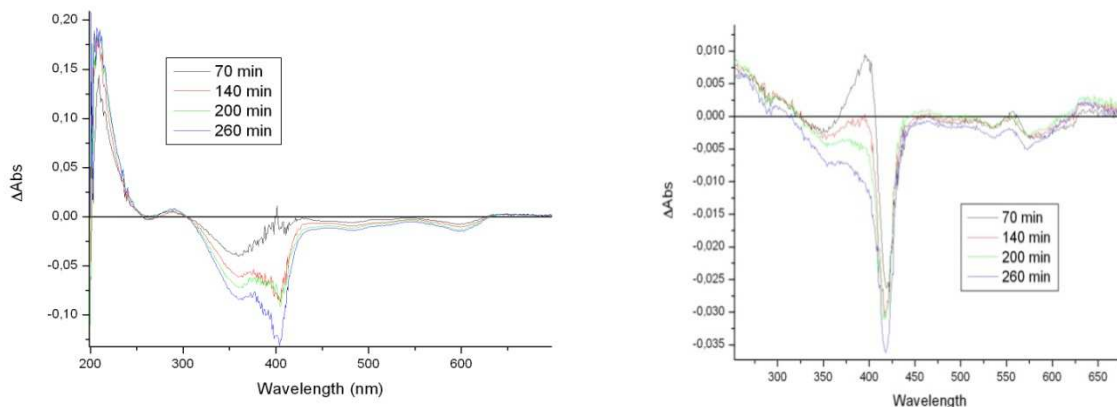


Figure 18, Difference spectra of cooled illumination of FePPIX (left, max abs 2) and CoPPIX (right, max abs 0.55) in methanol.

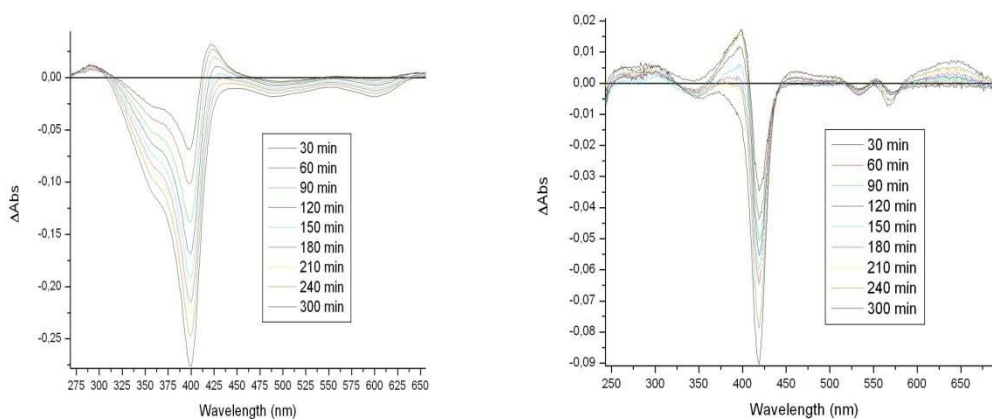


Figure 19, Difference spectra of cooled illumination of FePPIX (left, max abs 0.30) and CoPPIX (right, max abs 0.30) in methanol.

4.3. Porphyrins in colloidal solutions

Illumination of FePPIX anchored to TiO₂ in colloidal solution was performed in pyridine, DMSO and methanol while CoPPIX was examined in pyridine, methanol, DMSO and ethanol; however, ethanol and methanol samples with CoPPIX anchored to nanoparticulate TiO₂ are not presented in this report. Anchoring time was close to a full 24-hour period, which was assumed to be well beyond the time required for complete binding.

All but one colloidal solution samples were illuminated with a strong Xe-lamp with filters, which transmitted in the 330-350 nm region; the exception was FePPIX in methanol, which was illuminated by the monochromatic light from a Xe-lamp.

The molar ratio (M_R) between TiO₂ and MPPIX (i.e. [TiO₂]/[MPPIX]) might be important to the kinetics of the binding and possibly the number of MPPIX molecules that binds per particle.

FePPIX – Colloidal solution – Pyridine

The concentrations in the pyridine sample were: FePPIX 4.04 μM, TiO₂ 8.88 μM (M_R 2.2) and TBAPF₆ 0.1 M. The binding of FePPIX to TiO₂ were allowed to proceed for approximately 20 hours at which point TBAPF₆ were added and stirred for 30 min; the illumination started directly after this 30 min period. In Figure 20 we see a nearly instant change in the absorption, i.e. a red shift of the Soret band and an overall raise of the region ~475-575 nm. This change is subscribed to the change from Fe(III)PPIX to Fe(II)PPIX^[9], a conclusion which is supported by the isosbestic points at both sides of the Fe(II)PPIX Soret band, indicating that no destruction of the porphyrin is present. The ratio and direction of the increase/decrease is also consistent with literature values of (Py)₂Fe(II)PPIX^[9].

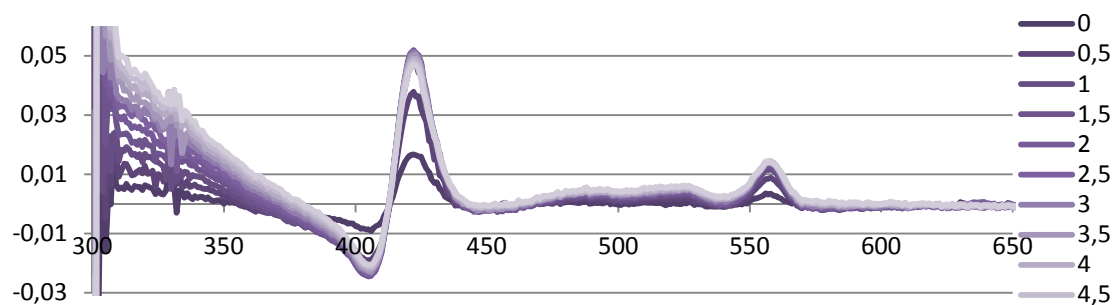


Figure 20, Difference spectra of illumination of FePPIX anchored to TiO₂ particles in pyridine with small amount of TBAPF₆ at different illumination times (time given in min), first 5 min.

Further illumination shows a small increase in absorbance of the Fe(II)PPIX Soret band until approximately 20 min, at which time it starts to decrease; possibly indicating the generation of Fe(I)PPIX accompanied by substantial destruction of the porphyrin, see Figure 21. The conclusion of destruction of the macrocycle is based on the overall decrease in absorption above ~380 nm. No tendency of populating the TiO₂ conduction band is seen.

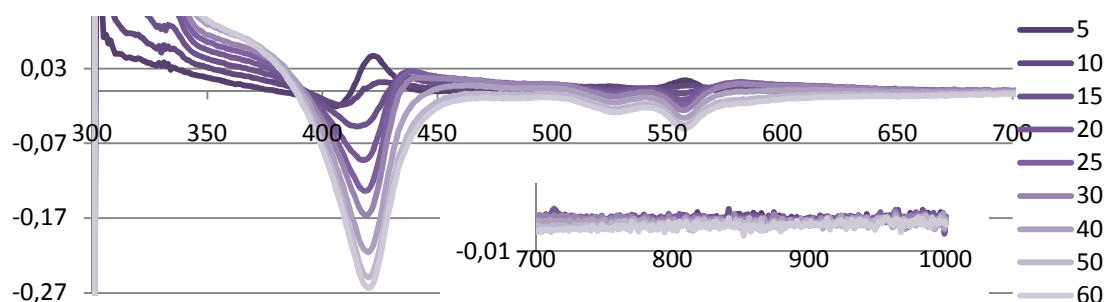


Figure 21, Difference spectra of continued illumination of FePPIX colloidal pyridine solution, first hour.

After illumination the sample was monitored over 9 hours to observe if the light induced change was reversible, see Figure 22. Initially, there were indications of a recovery process, but after about 15 minutes it came to an apparent halt.

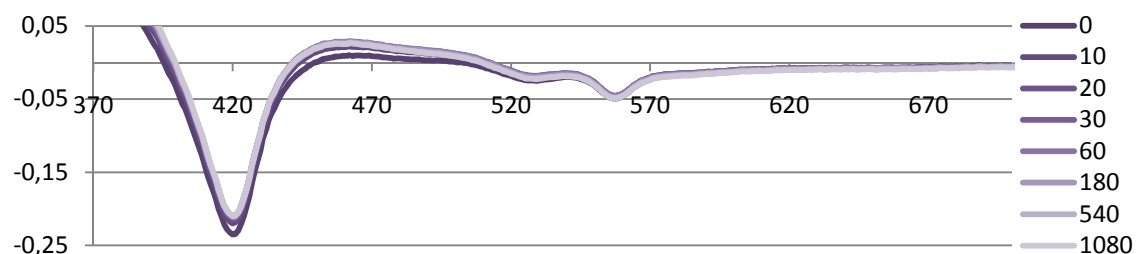


Figure 22, Difference spectra monitoring of the recovery of FePPIX in colloidal pyridine solution with $TBAPF_6$, time in min after the illumination was stopped.

The FePPIX-pyridine system is the only colloidal system that shows any tendency to recover at all after illumination, all the other recovery experiments in colloidal solution shows a slow, small decrease all over the spectrum and are not presented in this report.

FePPIX – Colloidal solution – Dimethyl sulfoxide

Illumination of FePPIX in DMSO with 0.1 M $TBAPF_6$ and a M_R of 3.6 resulted in a rapid reduction to Fe(II)PPIX before the spectrophotometer even finished through the first scan cycle (i.e. less than 20 sec). No further net reduction from Fe(III) to Fe(II) were seen, at this point either all Fe(III) were reduced or the rate of reduction/destruction of Fe(II) were larger.

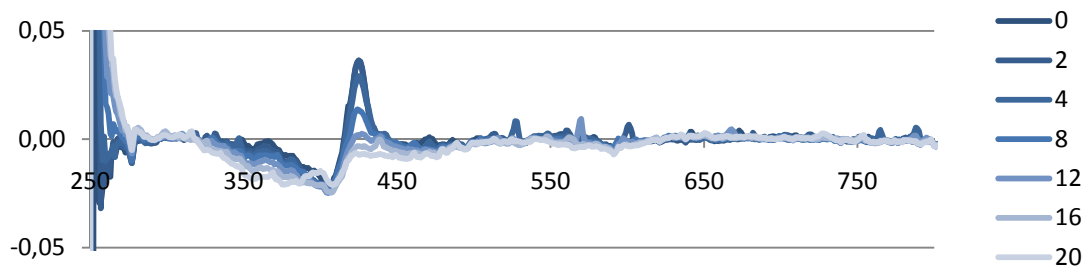


Figure 23, Difference spectra of the first 20 min of illuminating FePPIX in DMSO anchored to TiO_2 with 0.1 M $TBAPF_6$.

The isosbestic points rapidly disappeared, indicating further reduction or destruction of the porphyrin, see Figure 24; the latter is probably more likely as the resulting spectra is much alike a mirror image through the x-axis of the original spectrum. This is consistent with the experiments on FePPIX in neat DMSO, which also demonstrated indications of destruction of FePPIX when illuminated.

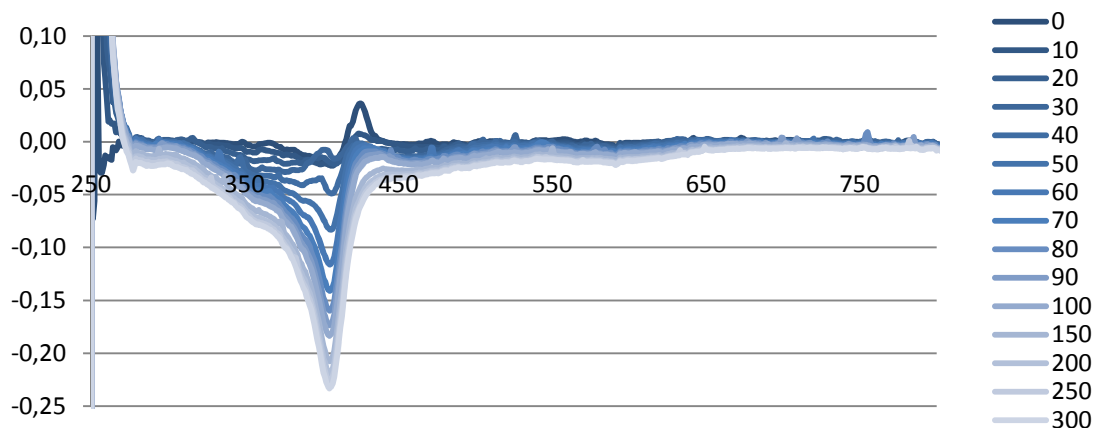


Figure 24, Difference spectra of the illumination of FePPIX anchored to TiO_2 in DMSO with 0.1 M $TBAPF_6$, time given in minutes.

FePPIX – Colloidal solution – Methanol

Instead of the pump light used in the other two samples with FePPIX in colloidal solution, a Q-switch laser was used in the methanol experiment. The behavior is very similar to that of FePPIX in colloidal DMSO solution, see Figure 25; i.e. initially a small fairly proportional red shift followed by a wide decrease of absorbance throughout the spectrum.

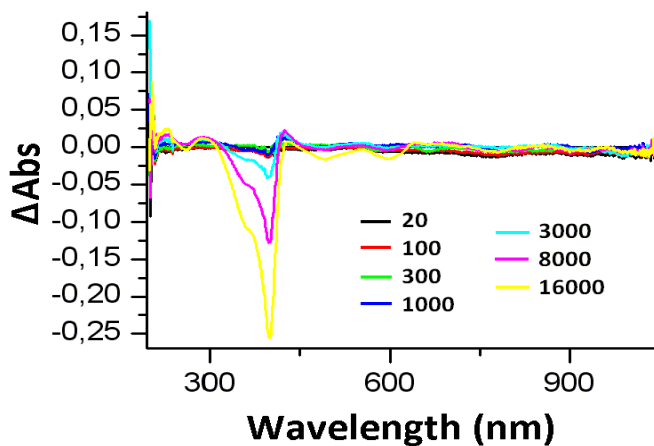


Figure 25, Pulsed illumination of FePPIX anchored to TiO_2 particles in methanol with 355 nm wavelength (pulswidth ca 10 nm FWHM).

CoPPIX – Colloidal solution – Pyridine

When CoPPIX in colloidal pyridine solution was illuminated there were two different apparent phases; the first five minutes the Soret band decreased followed by an absorption increase on both sides, further illumination resulted in an overall raise of the spectra below 700 nm, see Figure 26.

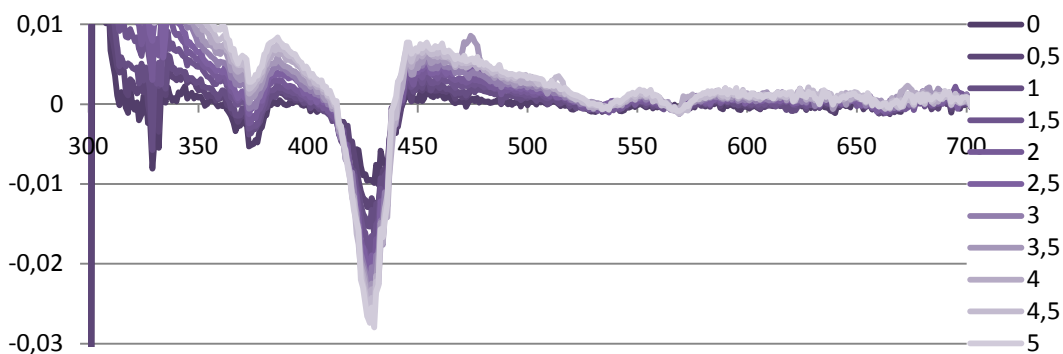
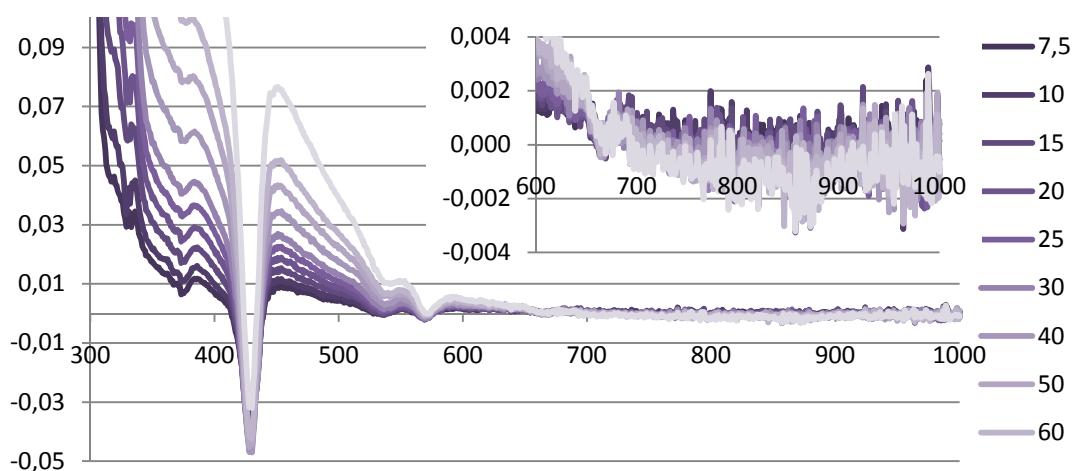


Figure 26, Difference spectra of illuminated CoPPIX anchored to nanoparticulate TiO_2 first 5 min (above) and first hour (below).



The first behavior is consistent with Co(III) reduction to Co(II) whereas the following raising of the whole spectra could indicate reduction to Co(I); for this to be true, the extinction coefficient for Co(I) must be higher than Co(II) at all wavelengths below 700 nm. This could be possible, but if CoPPIX's different redox states shares the appearance of FePPIX's ditto there should be another explanation.

The broad increase in absorbance is similar to addition of Rayleigh scattering active species; this could indicate aggregation of particles that were initially too small to scatter light in the Rayleigh fashion. Another factor that might contribute is the pump light intensity; even though an IR-filter was used to avoid excessive heating of the samples the temperatures were elevated. The temperature affects both reaction rates and solubility; as the pyridine samples had the highest concentrations of porphyrins this behavior can be a product of increased solubility of either porphyrins, TiO_2 or both.

CoPPIX – Colloidal solution – Dimethyl sulfoxide

When changing the ratio between CoPPIX and TiO_2 , the appearance of the illuminated samples spectra is changed as well, see Figure 27 and Figure 29. The reason of this is not known and further experiments on this topic were not performed.

In Figure 27 and Figure 29 one can see that the sample with higher nanoparticle concentration as a transient peak at 404 nm which reaches its maxima around 15 min. The isosbestic points hint that the peak is not due to a destruction product, instead it could mean that CoPPIX in DMSO is in the Co(II)PPIX state. This conclusion can be drawn by assuming CoPPIX and FePPIX extinction coefficient's features are similar when in the same state while consulting Table 3 and Table 4; CoPPIX in DMSO is very similar to Fe(II)PPIX in DMSO, it's also seen in Figure 28 that the intermediate species has a peak at 404 nm, which is the same as for Fe(III)PPIX in DMSO; furthermore, the similarities between the porphyrins in pyridine is very pronounced, the dissimilarity in values of extinction coefficients can be due to a real difference, to the solution storage time or the small amount of porphyrins measured on the scale when preparing samples.

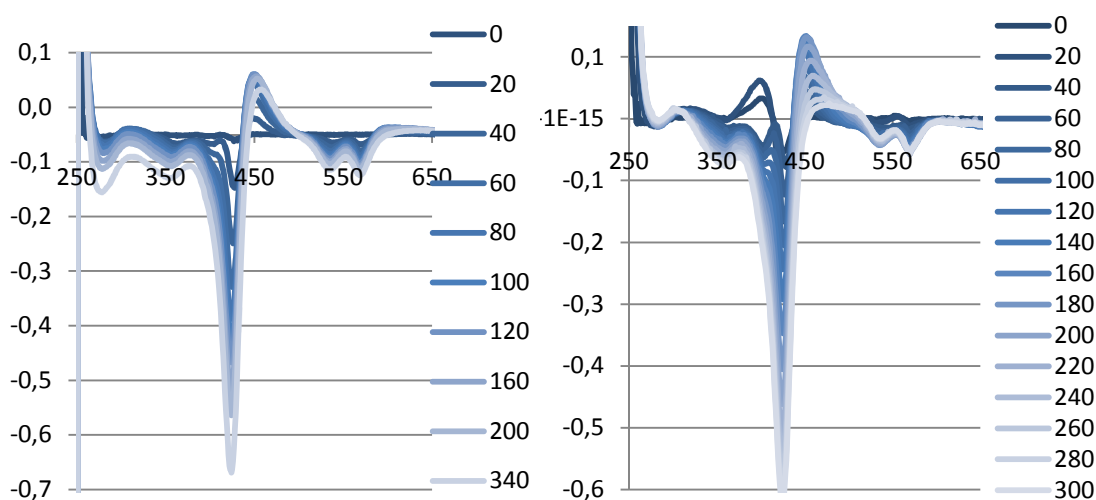


Figure 27, Difference spectra that compares illumination of CoPPIX anchored to TiO_2 with $M_R = 2.4$ (left) and $M_R = 38$ (right); time in min.

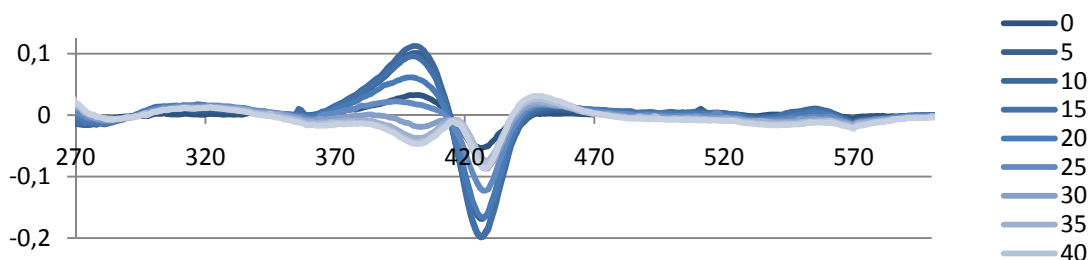


Figure 28, Difference spectra of the first 40 minutes of illumination upon CoPPIX anchored to nanoparticulate TiO_2 with $M_R = 38$.

4.4. Porphyrins anchored to TiO₂ thin films

To film samples in DMSO and pyridine a small amount, approximately 0.01-0.05 M, of TBAPF₆ was added; to the film in ethanol LiClO₄ were used, as the low solubility of TBAPF₆ in ethanol caused troubles in colloidal solution experiments.

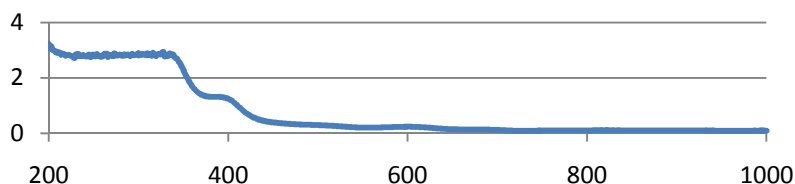


Figure 29, Absorbance spectra of FePPIX anchored to TiO₂ thin film in ethanol.

Thin films of TiO₂ absorb strongly in the UV-region, and due to scattering, the apparent absorbance values are even higher throughout the spectrum (see Figure 29 for illustration and recall Figure 8 about scattering) and the determination of bound porphyrin's concentration is not as straight forward as one might think. It is possible to measure the concentration of the dyeing solution before and after the immersion of the film; however, this does not account for any excess porphyrins rinsed away unless it's collected and measured as well. Furthermore, as the films are not completely homogenous, a problem of assessing the measured area's concentration arises. Extinction coefficients can be used, but is in practice difficult due to problems of establishing a baseline; local variations in the films were large and the only reasonable way of getting a baseline would be to stain the films in the spectrophotometer, to try and place them in the correct position after the baseline measurements have been tried and found to be very uncertain. A very large shift in absorbance was seen if the film was misplaced more than a fraction of a millimeter.

Between every illumination cycle in the film experiments there was a time delay of 30 seconds with no illumination; due to reflexes from the glass slides, simultaneous illumination and measuring was not possible.

FePPIX - Thin film - Ethanol

When FePPIX anchored to TiO₂ thin film with addition of a small amount of LiClO₄ in ethanol was illuminated, a very rapid change was observed, see Figure 30. The first measurement, after only 15 seconds of illumination, showed the greatest intensity at the Soret band of Fe(II); further illumination increased the absorbance of all wavelength above and a decrease those below 460 nm. The broad increase in absorption above 600 nm was assigned to electrons populating the conduction band of TiO₂ while the decrease in absorbance between 380 and 460 followed by a lesser increase between 460 and 600 nm is consistent with reduction of Fe(II) to Fe(I)^[2]. However, the generation of conduction band electrons should decrease if they were used to reduce Fe(II) to Fe(I), which means the light absorption of conduction band electrons in TiO₂ might start to absorb light around 470 nm, which would explain the spectral features. It is also reasonable to assume that the addition of Li⁺, a known potential determining ion^[4], would decrease the conduction band onset such that it becomes easier to promote

valance band electrons to it. Furthermore, if the conduction band is shifted enough, the energetic overlap with the reduction potential range will be smaller, and thus a huge number of conduction band electrons cannot be utilized for charge transfer despite their stability.

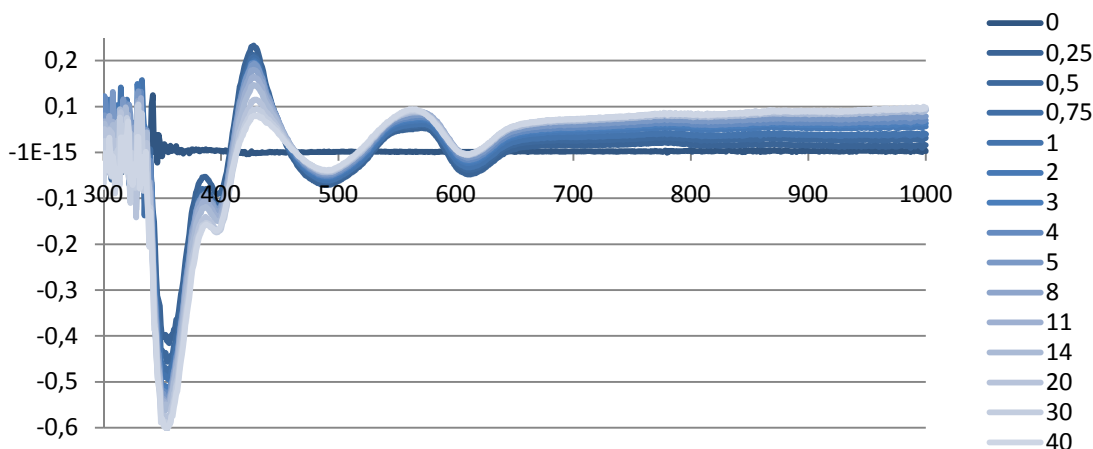


Figure 30, Difference spectra of illuminated FePPIX anchored to TiO_2 thin film in ethanol with a small addition of LiClO_4 , time given in minutes.

After illumination the recovery of the sample was monitored with the last illumination spectrum used as a baseline. Some recovery of the initial state was observed, see Figure 31; a comparison between the final state of Figure 30 and Figure 31, which to some extent are the mirror image of one another in the porphyrin range, leads us to this conclusion (observe that the y-axis in Figure 31 is inverted to simplify the visualization of the similarities). The recovery seems to follow the most expected pathway, i.e. Fe(I) to Fe(II) to Fe(III). Note that the conduction band electrons seem to be stable over long periods of time. By comparing of the values of the y-axis in Figure 30 and Figure 31 one can see that the illumination is reversible.

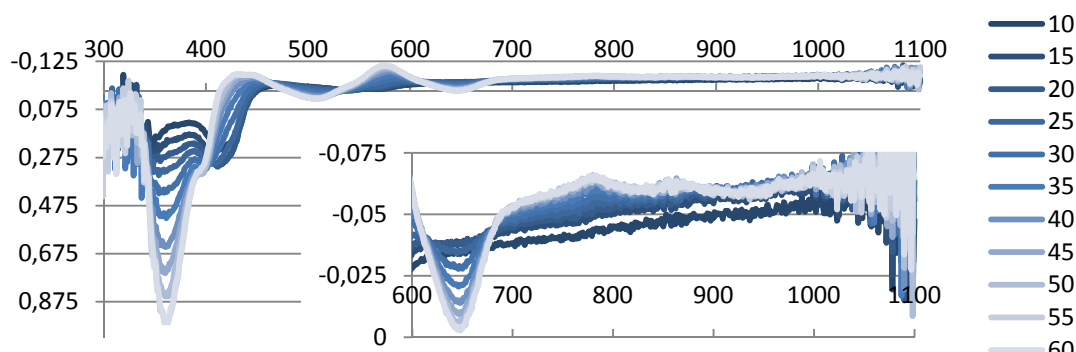


Figure 31, Difference spectra of illuminated FePPIX anchored to thin film monitoring the first hour of recovery. Observe the inverted order of the y-axis; this is done to simplify the comparison with the illumination spectra.

FePPIX - Thin film - DMSO

Illumination of FePPIX anchored to TiO_2 thin film generated a maximum Fe(II) Soret band after approximately 60 seconds, see Figure 33, further illumination seemed to reduce Fe(II) to Fe(I). The absorbance attributed to the conduction band of TiO_2 was elevated after 5 seconds (first measurement) and was stable until a large amount of Fe(II) was generated; kinetic studies

have shown that chromophore's excited-state electron injection to TiO_2 take place on pico- to femtosecond time-scale^[21]. If we examine the conduction band electron absorbance at 680 nm and compare it to the Soret band (424 nm), one could establish whether a certain concentration of conduction band electrons is necessary before any conduction band mediated processes can occur. In Figure 34 we see such a relationship, it's not a perfect overlap but the trends are similar.

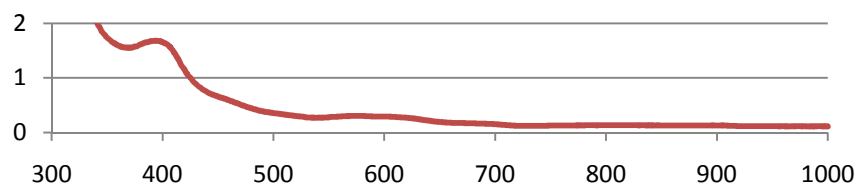


Figure 32, Baseline on non-illuminated FePPIX – Thin film – DMSO.

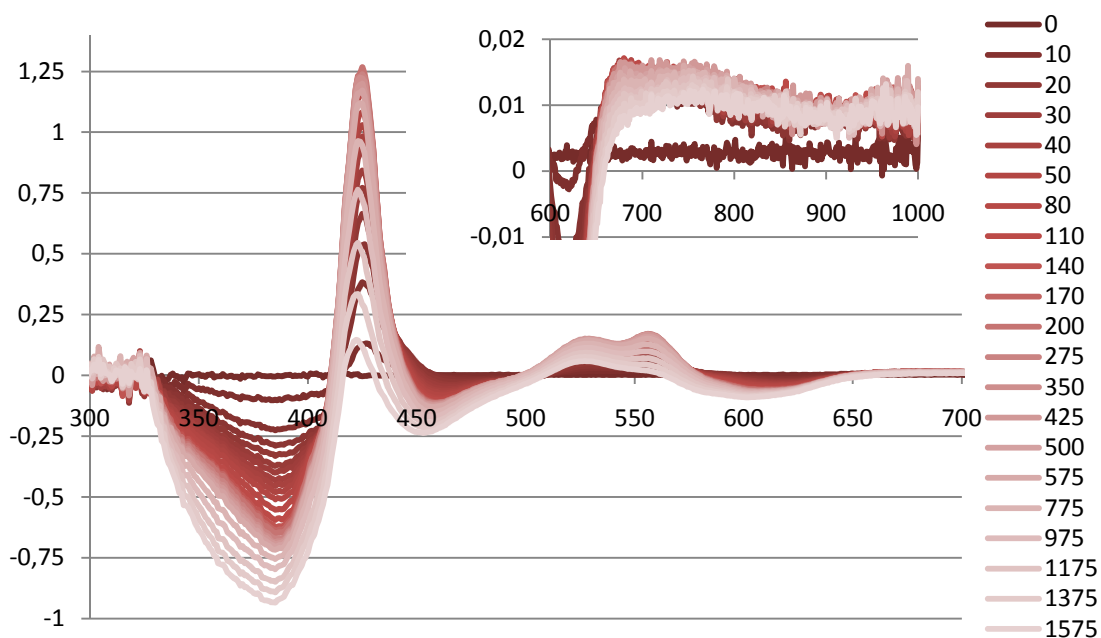


Figure 33, ΔAbs spectra of illuminated FePPIX anchored to TiO_2 thin film in DMSO, time in seconds; the labels of 5, 15, 25, 35 and 45 have been removed from the legend.

There was no increase in absorbance between 450 and 500 nm, indicating that Fe(I) is not generated, that destruction of porphyrins are proceeding at a higher rate than the generation of Fe(I) or that the Soret band of Fe(I)PPIX in DMSO is interlaced with Fe(II) with lower extinction coefficients over the measurement range. The test of reversibility is seen in Figure 35 and was monitored for 12 min. The recovery was proceeding for the whole time interval, this behavior and the coupled features in Figure 34 leads us to believe that Fe(I) is actually generated.

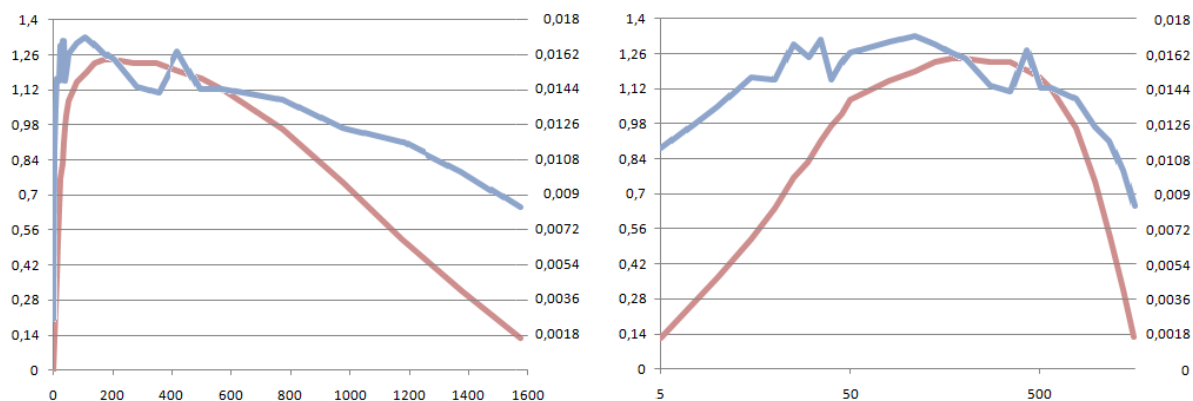


Figure 34, ΔAbs vs time (s) plotted for Soret band (424 nm, red, left axis) and for conduction band electrons (680 nm, blue, right axis); (Left) ΔAbs vs time [s], (Right) ΔAbs vs $\log(\text{time [s]})$.

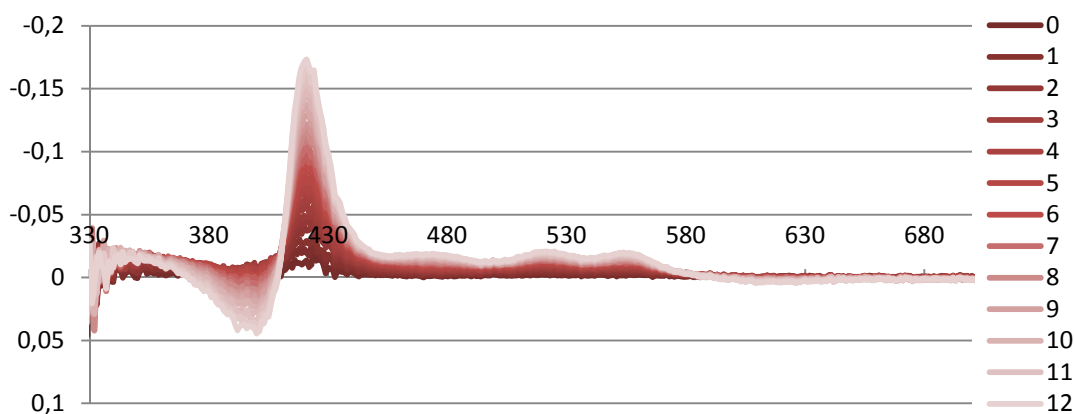


Figure 35, Difference spectra of the recovery of illuminated FePPIX anchored to TiO_2 thin film in DMSO, time in seconds; the labels of non integer minutes have been removed from the legend.

Observe the reversed order of the y-axis; this is done to simplify the comparison with the illumination spectra.

CoPPIX - Thin film - Ethanol

Illumination of CoPPIX anchored to TiO_2 thin films in ethanol with added $LiClO_4$ shared features with the corresponding experiment done with FePPIX; a promotion of valance band electron to the conduction band with time, fast reduction to Co(II) but no indication of Co(I) generation. Monitoring of the recovery (see Figure 37) indicated that the sample was able to return to the state it had before illumination; about 40% of the initial absorption had returned after 1000 minutes.

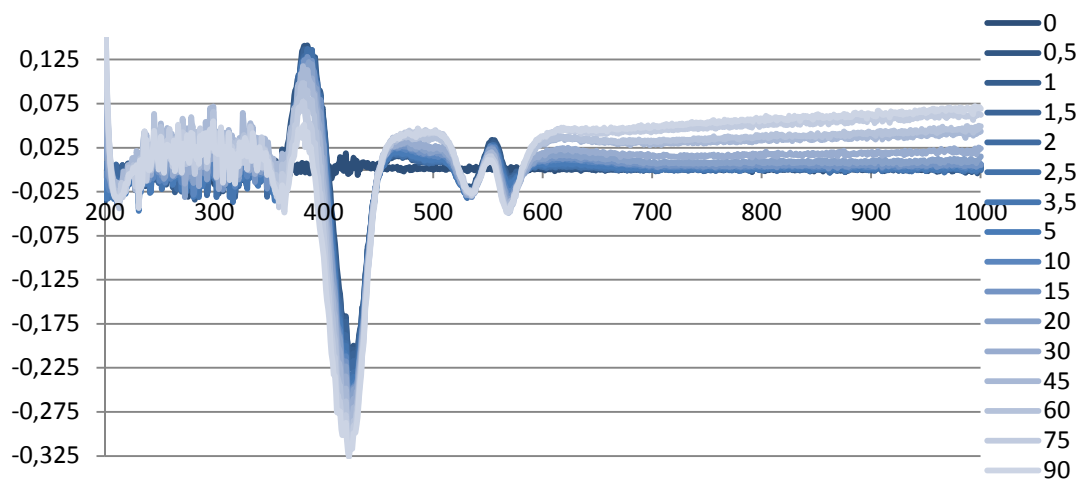


Figure 36, Difference spectra of illuminated CoPPIX anchored to TiO₂ thin film in ethanol, time in minutes.

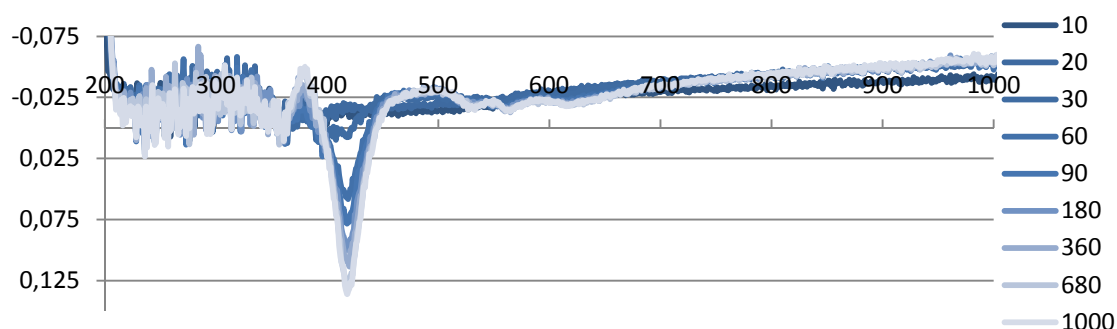


Figure 37, Difference spectra monitoring the recovery of illuminated CoPPIX anchored to TiO₂ thin film in ethanol, time in minutes; observe that the y-axis is inverted.

CoPPIX –Thin film - Pyridine

The trend seen when CoPPIX was anchored to TiO₂ thin film in pyridine was very similar to the case where ethanol was used.

A dyed film in pyridine was used to monitor the stability of the bond between TiO₂ and the porphyrin. After dyeing the thin film, it was put in neat pyridine and monitored over time; if the concentration of porphyrins in the solvent and on the film has an equilibrium character, a decrease in absorbance should have been seen. However, the absorbance is, within the experiment's time frame, rather stable. Some indication of reduction of the complex is seen, but to a very limited extent.

After storing the film in solvent for a week, under ambient conditions, the solution became colored. No measurement was performed, but it is evident the binding is not stable forever.

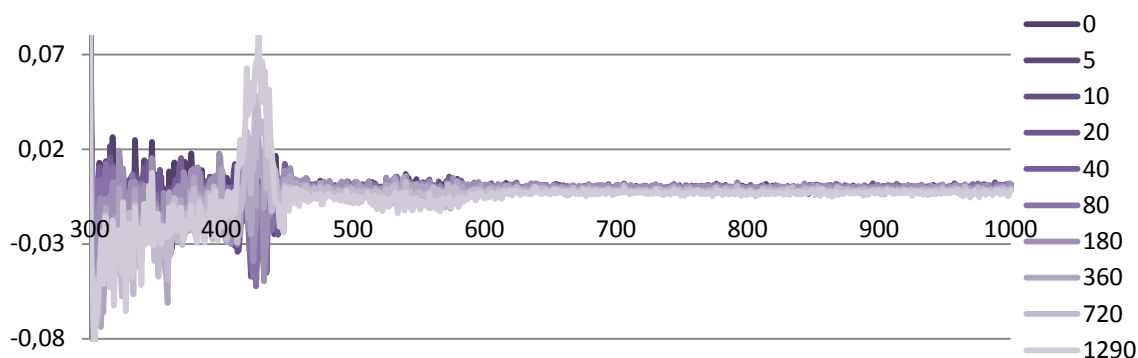


Figure 38, Difference spectra, a stability test of the binding between the TiO_2 thin film and CoPPIX after 50 min of dyeing, time in minutes.

4.5. Anchoring of porphyrins to nanoparticular TiO_2

FePPIX was added to neat pyridine to a concentration of $4.04 \mu\text{M}$; the solution was purged with N_2 for 30 min. A baseline was recorded and after an addition of nanoparticular TiO_2 , the effect of binding between FePPIX and TiO_2 was monitored; the max absorbance before addition of TiO_2 was ~ 1.2 .

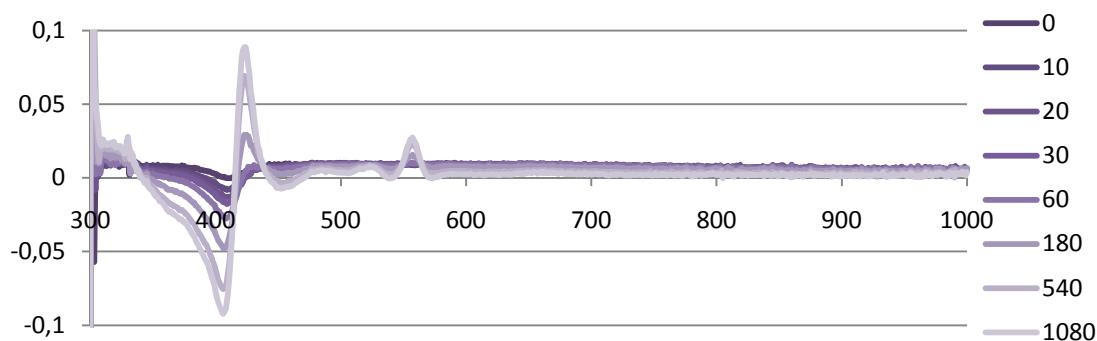


Figure 39, ΔAbs spectra depicting the behavior of FePPIX ($4.04 \mu\text{M}$) in pyridine upon addition of nanoparticular TiO_2 ($8.8 \mu\text{M}$).

The behavior seen in Figure 39 is consistent with the reduction of Fe(III)PPIX to Fe(II)PPIX, indicating either that the binding process can reduce the porphyrin or that there are a mixture of Fe(II) and Fe(III) in pyridine solution. Recalling the extinction coefficient experiments, the extinction coefficient of FePPIX's Soret band in pyridine is considerably red shifted compared to the corresponding peak in DMSO and methanol; this can be explained if the Fe(II) state in pyridine is favored over the Fe(III) state. It has been previously observed that autoreduction processes can occur in pyridine^[22] and this might be the reason for this observed behavior.

4.6. Nanoparticulate TiO₂ in neat solution

4.6.1. Illumination of TiO₂ in neat solvent

TiO₂ particles in methanol was exposed to pulsed laser light, 355 nm, measured at 20, 100, 300, 1000, 3000 and 7000 pulses; the resulting difference spectra is visible in Figure 40. As the sample contained particles, and colloidal solution of methanol and TiO₂ sooner or later gets unstable^[18a], some aggregation probably occurred; this should not have been enough to affect the trend visible in Figure 40, although it increased the noise.

The baseline was shifting, which is most probable caused by the shaking of the sample to prevent sedimentation, and rendered the measurements reliability lower for quantitative conclusions; it can however be used for qualitative studies. The obvious trend, the shifting baseline excluded, was a raise of the absorption in the red and near infrared region, indicating a populated conduction band in the TiO₂. Even though the baseline shift made a quantitative statement less reliable, the populating rate is rather low compared to e.g. film experiments.

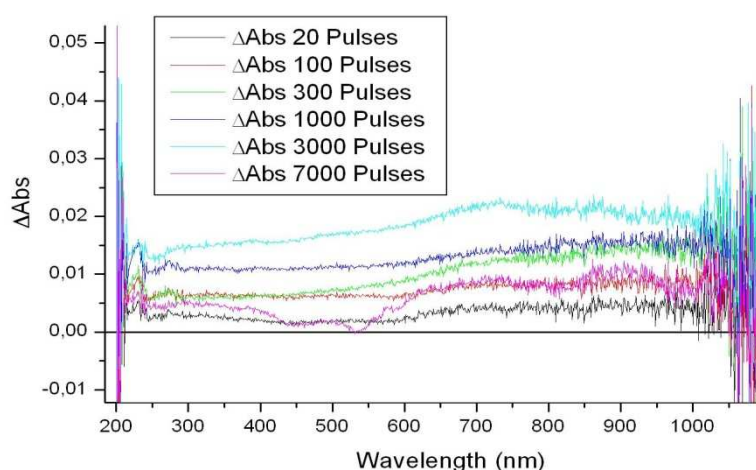


Figure 40, Pulsing of TiO₂ particles in MeOH with 355 nm laser (50 μ s pulses), absolute absorbance values for the 400-1100 region \sim 0.2.

4.6.1. Sedimentation of TiO₂ in neat methanol

The sedimentation experiment, performed in neat methanol, showed an almost linear ($R^2=0.983$) decrease of absorbance corresponding to around 3-4% in 20 min. After 2 hours the sample was rigorously shaken and remeasured, the max intensity had decreased by 0.5% and the sedimentation after shaking showed high resemblance with the first measurement.

The conclusion from the sedimentation experiment is that the aggregation rate is low enough for viable experiment in a timescale of at least several hours; assuming that the sample is stirred. However, the sedimentation in illuminated samples was not performed; samples with altered charge distribution, e.g. excited, with additives or anchored molecules, can behave differently. Thus, irreversible aggregation in other solvent and/or environment is not dismissed.

5. Discussion

Comparison between TiO₂ thin films and TiO₂ colloidal solutions

Comparisons between thin film and colloidal solution experiments indicate that for conduction band mediated charge transfer processes, thin film assemblies are preferred. The photoinduced generation of conduction band electrons is only visible in the film experiments and, more importantly, the rate of photoinduced reduction of the porphyrins is also considerably higher in thin films. This could be due to high concentration of CB electrons unutilized by the porphyrins while colloidal solution experiment was unable to produce the concentration of CB electrons needed, however, since the rates of the build-up were not examined in detail, the critical concentration of conduction band electrons needed for CB mediated charge transfer to occur is not known. It should also be noted that there might be conduction band electrons in the colloidal case, but they might be so short-lived that they were undetectable under the conditions used here.

The reversibility of the light induced catalytically active state is also of importance; in colloidal solution virtually no recovery was observed while the opposite holds true for the thin films. A high rate of recovery can be an indication of reactions between the porphyrins and substances in the sample, i.e. the porphyrin is in a catalytically active state.

For future possible industrial uses, there are several parameters to consider that does not cause problems on lab scale. The fact that films does not suffer from the drawbacks with colloidal solutions, e.g. aggregation, need of continuous stirring and problems with low solubility, also speaks in favor of choosing films over colloidal solution for catalysis on larger scales. Also, if the proposed reactants or products in the catalytic reaction are liquid, a recovery step for catalyst in colloidal solution would be needed (energy demanding); in comparison, a catalyst attached to a surface should suffer less net loss of catalyst mass. If the reactants are in gaseous phase, the solubility of the gas could limit the efficiency of solution catalysis while gas phase catalysis could possibly be carried out with thin films.

If it is possible to achieve greater photoinduced generation of conduction band electrons in colloidal solution by altering the size and environment of the particles, the colloidal solution could be more desirable than thin films due to the distribution of particles in solution; compared to thin films, where the catalysis is only carried out in a thin layer. This however needs to be investigated further.

Comparison between FePPIX and CoPPIX

FePPIX and CoPPIX anchored to thin films and nanoparticles have shown similar behaviors when illuminated; the big difference between them is the stability in neat solution, both in terms of stability under continuous illumination and in terms of solubility.

There are also indication that the wavelength of the different porphyrins are coupled; Fe(III) resembles Co(II), the latter seems to be the most common state of CoPPIX in neat solution. As the generation of the different redox states has been carried out under similar condition, it should mean that the energy level needed for reduction of Fe(III) should correspond to the

reduction of Co(II); this can possibly cause problems if further reduction is needed, i.e. Fe(0)/Co(-1).

6. Summary and outlook

6.1. Summary

This work has confirmed the occurrence of conduction band mediated charge transfer in nanocrystalline TiO₂ thin films when illuminated with UV-light under steady state conditions. However, this observation could not be confirmed in colloidal solution of TiO₂ nanoparticles. Reduction from Fe(III) in two steps to Fe(I) is seen in thin film samples immersed in DMSO and pyridine, with further tuning of TiO₂ one could get faster rates and *possibly* reduction to Fe(0).

Thin films with anchored porphyrin immersed in solvent containing Li⁺ shows a large build-up of CB electrons. However, a second reduction of the porphyrins is not visible, indicating that the overlap between the CB energy level and the reduction potential for the second reduction of porphyrins has diminished.

Thus semiconductor thin films should be the preferred choice when proceeding with this project, using conduction band mediated charge transfer to generate highly reduced catalytically active states.

- Films showed higher tendency of conduction band electrons build-up.
- Films showed faster rates and more complete reduction of the model catalysts.
- Films showed higher reversibility of the system compared to colloidal solution.
- Porphyrins bound to films were more stable than those attached to colloidal particles.
- Films are less problematic to work with, which could possibly be helpful for future up-scaling.

6.2. Outlook

A set of spectroelectrochemical experiments should be performed to better characterize the spectral features of the various redox states of the porphyrins; some parameters that needs to be evaluated are e.g. the extinction coefficients of different states, redox potentials and band conduction band onset.

The extinction coefficients alone would allow already obtained data to reveal more information, e.g. conversion ratios and the reversibility of the reactions.

Furthermore, extensive kinetic studies have to be performed to investigate how different additives and solvent combinations affect rates and recovery so that the conduction band mediated processes can be controlled.

Another important task of the project is to examine the effect of bound sensitizers upon photoinduced conduction band electrons in TiO₂. The natural follow up of this would be simultaneous binding of sensitizers and catalyst.

7. Acknowledgements

First of all I would like to thank **Maria** for taking me in and introducing me to this wonderful place, for all our enlightening discussion, for always letting me think aloud, for all the encouraging words and for your patience with my optimistically view on time.

I would also like to thank **Melina** for all the help she has provided me with equipment and all our discussions, pointing me in the right direction.

A thank you to **Jesper** as well, for help with equipment and for lending me small but important things.

I also like to thank all **master thesis workers**, for all the laughter, the pranks, the pleasant mood and for the sense of belonging.

I would also like to thank **all the other persons at the department** I've encountered during the time I've been here, for the warm reception and interesting discussions. An extra thanks also to the **spring party committee** for a lovely evening.

Another big thanks to **Emelie**, who has put up with me and tried to reminded me of the importance of regular eating and a good night's sleep, thank you for your love and support.

References

- [1] W. Cramer, A. Bondeau, S. Schaphoff, W. Lucht, B. Smith and S. Sitch, *Philosophical Transactions of the Royal Society of London Series B-Biological Sciences* **2004**, 359, 331-343.
- [2] M. Abrahamsson in *Nanoscopic photocatalytic assemblies: Photophysical, photochemical & photocatalytic properties of transition metal compounds.*, Vol. Göteborg, **2010**.
- [3] E. A. M. Lesley E. Smart in *Solid state chemistry An introduction*, Vol. 3 Taylor & Francis Group, Boca Raton, **2005**.
- [4] A. Staniszewski, A. J. Morris, T. Ito and G. J. Meyer, *Journal of Physical Chemistry B* **2007**, 111, 6822-6828.
- [5] a) I. Bhugun, D. Lexa and J. M. Saveant, *Journal of the American Chemical Society* **1996**, 118, 3982-3983; b) S. O. Obare, T. Ito and G. J. Meyer, *Journal of the American Chemical Society* **2006**, 128, 712-713.
- [6] M. B. Grazyna Stochel, Wojciech Macyk, Zofia Stasicka, Konrad Szacilowski in *Bioinorganic Photochemistry*, Vol. 1 John Wiley & Sons, Ltd., Hong Kong, **2009**.
- [7] S. Ardo and G. J. Meyer, *Chemical Society Reviews* **2009**, 38, 115-164.
- [8] R. S. Tieman, L. A. Coury, J. R. Kirchoff and W. R. Heineman, *Journal of Electroanalytical Chemistry* **1990**, 281, 133-145.
- [9] G. J. Meyer, A. J. Morris and J. R. Stromberg, *Inorganic Chemistry* **2010**, 49, 29-37.
- [10] S. W. Ryter and R. M. Tyrrell, *Free Radical Biology and Medicine* **2000**, 28, 289-309.
- [11] O. W. Kolling, *Journal of Physical Chemistry* **1989**, 93, 3436-3439.
- [12] D. F. Watson, A. Marton, A. M. Stux and G. J. Meyer, *Journal of Physical Chemistry B* **2004**, 108, 11680-11688.
- [13] J. R. Stromberg, J. D. Wnuk, R. A. F. Pinlac and G. J. Meyer, *Nano Letters* **2006**, 6, 1284-1286.
- [14] S. Pelet, J. E. Moser and M. Gratzel, *Journal of Physical Chemistry B* **2000**, 104, 1791-1795.
- [15] I. Bhugun, D. Lexa and J. M. Saveant, *Journal of the American Chemical Society* **1996**, 118, 1769-1776.
- [16] J. M. Hollas in *Modern Spectroscopy*, Vol. 4 John Wiley & Sons Ltd., Chichester, **2004**.
- [17] S. Wartewig in *IR and Raman Spectroscopy: Fundamental Processing.*, Vol. 1 WILEY-VCH GmbH & Co. KGaA, Weinheim, **2003**.
- [18] a) S. O. Obare, T. Ito and G. J. Meyer, *Environmental Science & Technology* **2005**, 39, 6266-6272; b) S. O. Obare, T. Ito, M. H. Balfour and G. J. Meyer, *Nano Letters* **2003**, 3, 1151-1153.
- [19] R. W. Larsen, J. Murphy and E. W. Findsen, *Inorganic Chemistry* **1996**, 35, 6254-6260.
- [20] J. Grodkowski, D. Behar, P. Neta and P. Hambright, *Journal of Physical Chemistry A* **1997**, 101, 248-254.
- [21] D. F. Bocian, J. R. Stromberg, A. Marton, H. L. Kee, C. Kirmaier, J. R. Diers, C. Muthiah, M. Taniguchi, J. S. Lindsey, G. J. Meyer and D. Holten, *Journal of Physical Chemistry A* **2007**, 111, 15464-15478.
- [22] A. L. Balch, B. C. Noll, M. M. Olmstead and S. L. Phillips, *Inorganic Chemistry* **1996**, 35, 6495-6506.

Appendix – Extinction coefficients

CoPPIX in DMSO

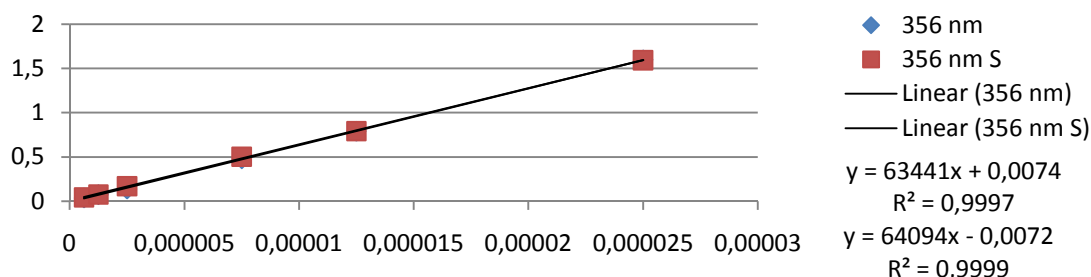


Figure 41, CoPPIX in DMSO, absorbance versus concentration (M) at 356 nm shoulder. S stands for shaken sample; the different samples were used to check the solubility of CoPPIX in DMSO.

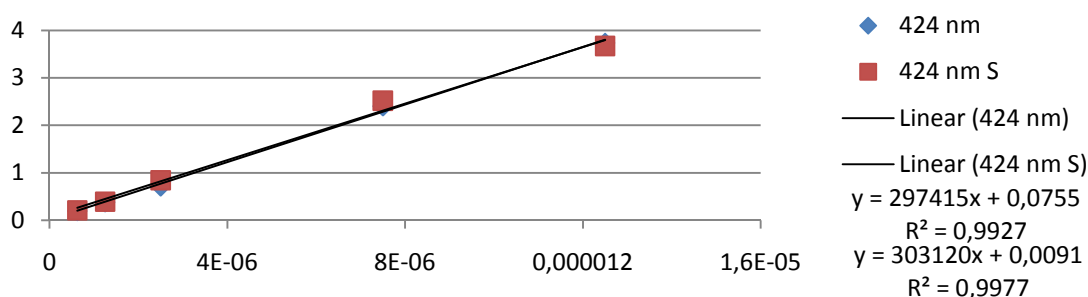


Figure 42, CoPPIX in DMSO, absorbance versus concentration (M) at 424 nm Soret band.

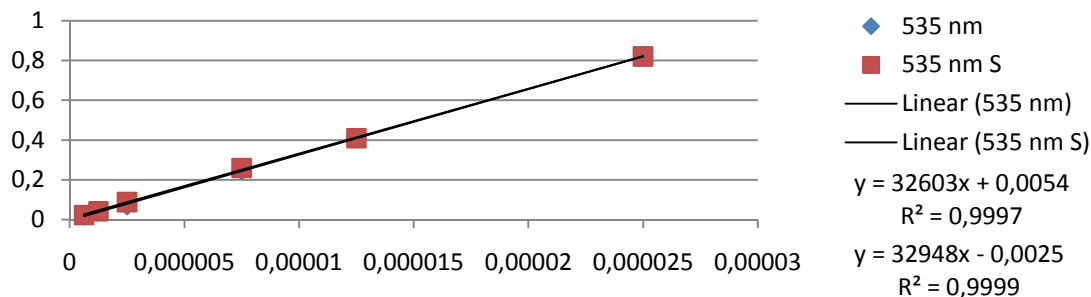


Figure 43, CoPPIX in DMSO, absorbance versus concentration (M) at 535 nm α band.

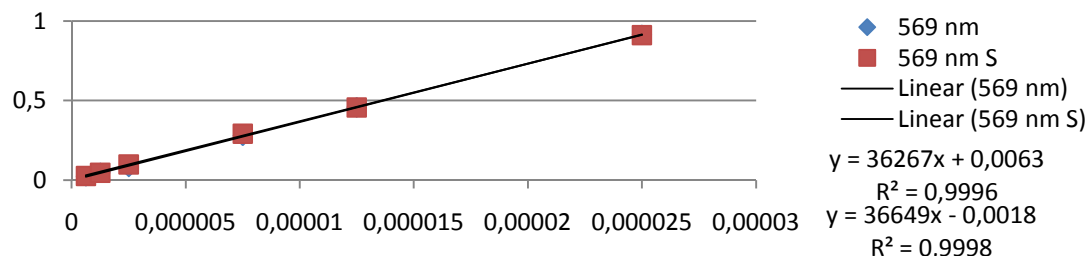


Figure 44, CoPPIX in DMSO, absorbance versus concentration (M) at 569 nm β band.

CoPPIX in methanol

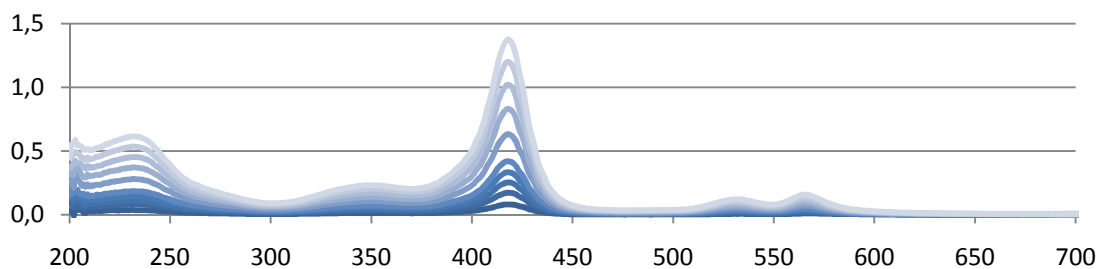
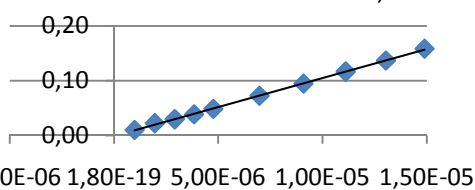


Figure 45, CoPPIX in methanol; concentration 0.990, 1.961, 2.913, 3.846, 4.762, 6.978, 9.091, 11.11, 13.04 and 14.89 μM .

565 nm

$$y = 10589x - 0,0011$$

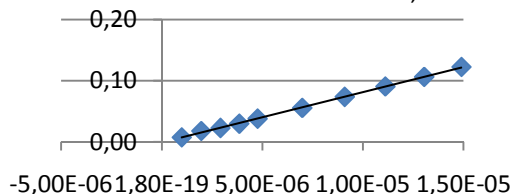
$$R^2 = 0,9995$$



531 nm

$$y = 8229,5x - 0,0008$$

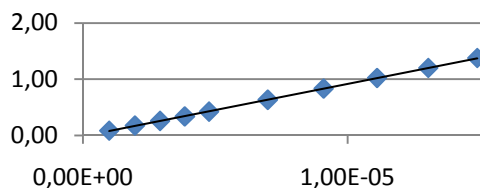
$$R^2 = 0,9993$$



418 nm

$$y = 93273x - 0,0163$$

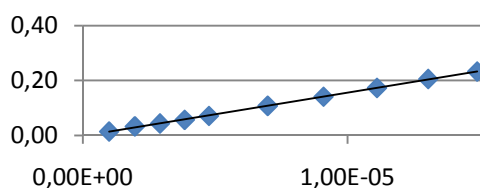
$$R^2 = 0,9999$$



351 nm

$$y = 15760x - 0,0018$$

$$R^2 = 0,9995$$



232 nm

$$y = 41566x - 0,007$$

$$R^2 = 0,9996$$

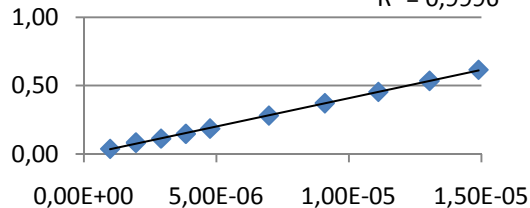


Figure 46, Absorbance versus concentration at (top left) β -band, (top right) α -band, (mid left) Soret band, (mid right) shoulder and UV-region peak (bottom).

CoPPIX in pyridine

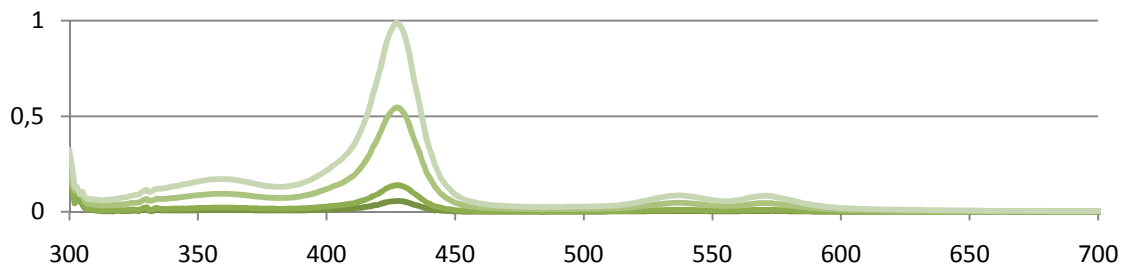


Figure 47, CoPPIX in pyridine; concentration 0.895, 1.79, 5.37 and 8.95 μM .

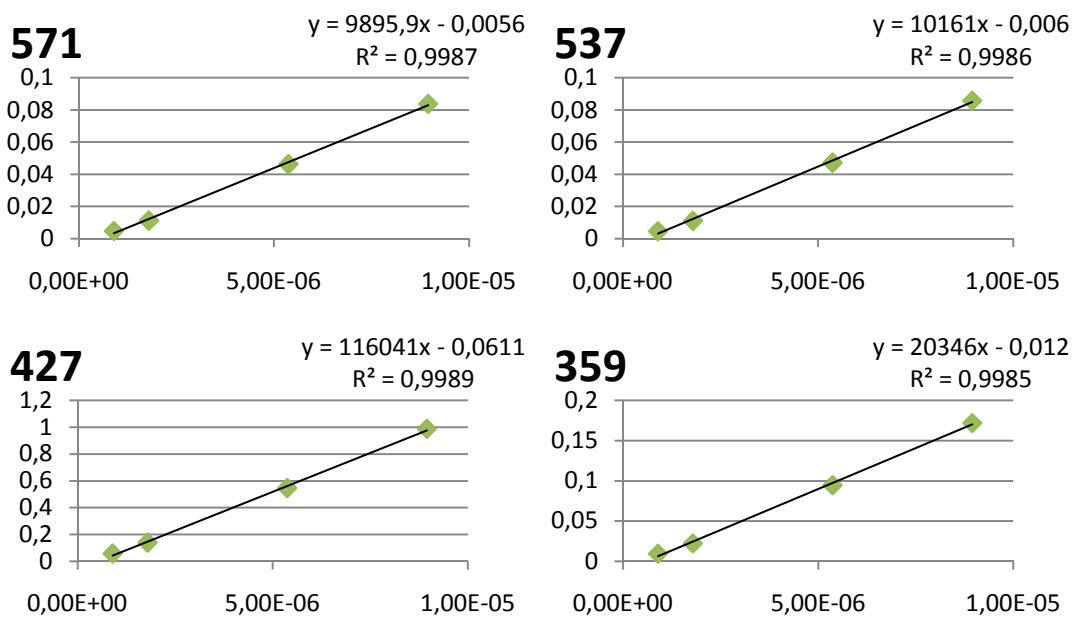


Figure 48, Absorbance versus concentration at (top left) β -band, (top right) α -band, (low left) Soret band and (low right) shoulder.

FePPIX in pyridine

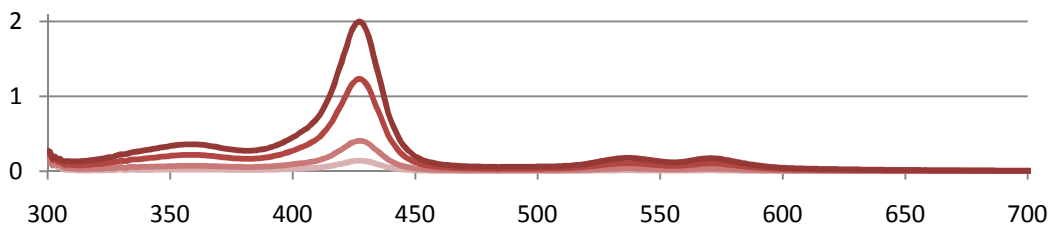


Figure 49, FePPIX in pyridine; concentration 0.730, 1.345, 4.035 and 6.730 μM .

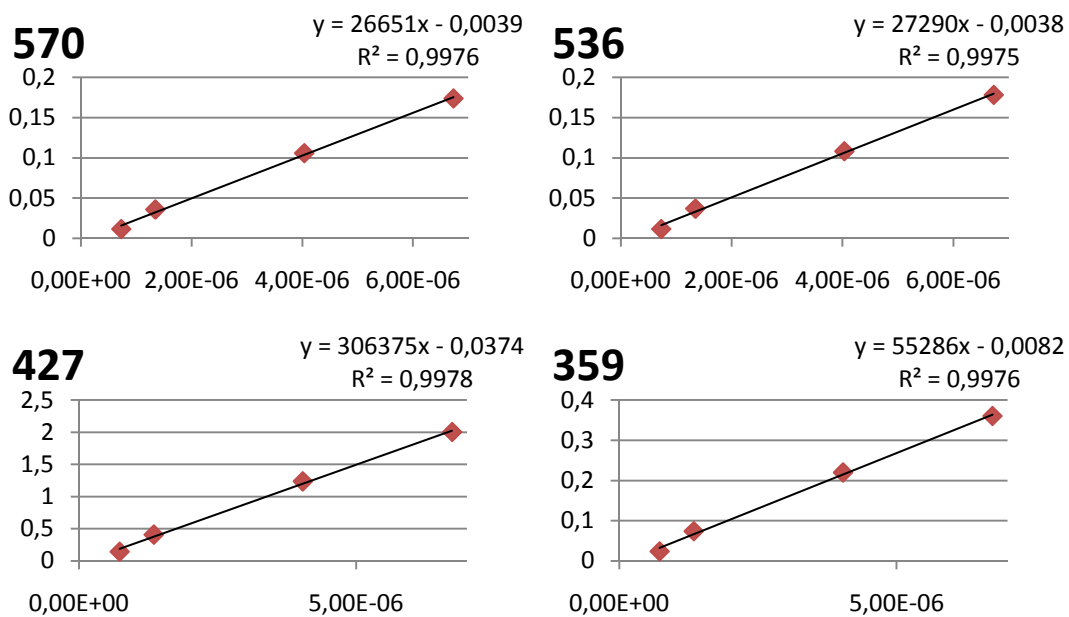


Figure 50, Absorbance versus concentration at (top left) β -band, (top right) α -band, (low left) Soret band and (low right) shoulder.